Renewable and Sustainable Energy Reviews 202 (2024) 114620

Contents lists available at ScienceDirect

Renewable and Sustainable Energy Reviews

journal homepage: www.elsevier.com/locate/rser

Original Research Article

Optimal sizing of renewables-to-hydrogen systems in a suitable-site-selection geospatial framework: The case study of Italy and Portugal

Leonardo Vidas [a,*], Rui Castro [b], Alessandro Bosisio [c], Armando Pires [d]

[a] Instituto Superior Técnico, University of Lisbon, Lisbon, Portugal
[b] INESC-ID/IST, University of Lisbon, Lisbon, Portugal
[c] University of Pavia, Pavia, Italy
[d] SustainRD, EST Setúbal, Polytechnic Institute of Setubal, Setubal, Portugal

ARTICLE INFO

Keywords:
Hydrogen
Renewable energy sources
Geospatial analysis
Optimisation
Hybrid power systems
Sensitivity analysis

ABSTRACT

Growing renewable energy deployment worldwide has sparked a shift in the energy landscape with far-reaching geopolitical ramifications. Hydrogen's role as an energy carrier is central to this change, facilitating global trade and the decarbonisation of hard-to-abate sectors. This analysis offers a new method for optimally sizing solar/wind-to-hydrogen systems in specifically suitable locations. These locations are limited to the onshore and offshore regions of selected countries, as determined by a bespoke geospatial analysis developed to be location-agnostic. Furthermore, the research focuses on determining the best configurations for such systems that minimise the cost of producing hydrogen, with the optimisation algorithm expanding from the detailed computation of the classic levelised cost of hydrogen. One of the study's main conclusions is that the best hybrid configurations obtained provide up to 70% cost savings in some areas. Such findings represent unprecedented achievements for Italy and Portugal and can be a valuable asset for economic studies of this kind carried out by local and national governments across the globe. These results validate the optimisation model's initial premise, significantly improving the credibility of this work by constructively challenging the standard way of assessing large-scale green hydrogen projects.

1. Introduction

The expanding deployment of renewables has put in motion a global energy revolution with profound geopolitical implications. The coming of a new energy age will transform relationships between nations and communities and create a new world of power security, energy independence and human prosperity. Unlike fossil fuels, whose reserves are concentrated in specific regions, renewable energy sources (RES) are available in every country. Since renewable energy can be produced anywhere, it has the potential to significantly alter the way that energy is traded. However, no viable and economical method for long–distance renewable electricity transportation has been established. Green hydrogen might provide a solution—as an energy carrier, hydrogen allows the trading of renewable energy across continental and regional borders. It also makes the decarbonisation of harder–to–abate sectors (such as the heavy steel and cement industries) easier. Hence, hydrogen has been recognised as a leading study subject, driven by unprecedented policy focus and put on the spotlight to investors and other market players [1].

Stemming from and subsequent to this recent surge in interest, academia has seen a growing body of research being published containing hydrogen–related keywords. This work intends to contribute to said groundwork by exploring the feasible linkages of hydrogen systems directly coupled to RES.

Hydrogen technologies have gone through many cycles of expectation over the last decades. Although the vast majority of hydrogen produced to date has come from steam methane reforming, the production through green electrolysis has grown considerably—mostly driven by hydrogen road–maps enacted by governments around the globe [2]. Efforts exist to ramp the up–scaling of electrolysers for high–purity hydrogen production, supported by recommendations by the International Energy Agency (IEA); some suggest that it is not beneficial to connect all this capacity to the electric grid, which is facing enough of a challenge keeping up with the increase in demand for electrification [3]. A solution could come from systems with increasing shares of variable renewable energy sources, where low–cost surplus electricity may be available. The authors considered the environmental consequences of the overall system and the comparison of economic factors with existing

* Corresponding author.
E-mail address: leonardo.vidas@tecnico.ulisboa.pt (L. Vidas).

https://doi.org/10.1016/j.rser.2024.114620
Received 18 December 2023; Received in revised form 12 May 2024; Accepted 1 June 2024
Available online 15 June 2024
1364-0321/

Abbreviations

AlkEl	**alk**aline **el**ectrolyser
AEMEl	**a**nion **e**xchange **m**embrane **el**ectrolyser
BOS	**b**alance **o**f **s**ystem
CapEx	**cap**ital **ex**penditures
CFEl	**c**apillary–**f**ed **el**ectrolyser
CRS	**c**oordinate **r**eference **s**ystem
DecEx	**dec**ommission **ex**penditures
DEM	**d**igital **e**levation **m**odel
EEZ	**e**xclusive **e**conomic **z**one
EU	**E**uropean **U**nion
EUR	**Eur**o
EPSG	**E**uropean **P**etroleum **S**urvey **G**roup
FLH	**f**ull **l**oad **h**ours
GBP	**G**reat **B**ritain **P**ound
GCR	**g**round **c**over **r**atio
GIS	**g**eographic **i**nformation **s**ystem
IEA	**I**nternational **E**nergy **A**gency
IRENA	**I**nternational **R**enewable **En**ergy **A**gency
LCOE	**l**evelised **c**ost **o**f **e**lectricity
LCOH	**l**evelised **c**ost **o**f **h**ydrogen
NPV	**n**et **p**resent **v**alue
NREL	**N**ational **R**enewable **E**nergy **L**aboratory
OGM	**o**ptimised **g**eneral **m**odel
O&M	**o**perations and **m**aintenance
OpEx	**op**erational **ex**penditures
PEMEl	**p**roton **e**xchange **m**embrane **el**ectrolyser
PV	**p**hoto**v**oltaic
ReplEx	**repl**acement **ex**penditures
RES	**r**enewable **e**nergy **s**ources
RC	**r**oughness **c**lass
SGM	**s**implified **g**eneral **m**odel
SOEl	**s**olid **o**xyde **el**ectrolyser
USD	**U**nited **S**tates **D**ollar
UTM	**U**niversal **T**ransverse **M**ercator
VAT	**v**alue **a**dded **t**ax
WACC	**w**eighted **a**verage **c**ost of **c**apital
WGS 84	**W**orld **G**eodetic **S**ystem 19**84**
yr	**y**ea**r**

Nomenclature

Blackboard bold typefaces

$\mathbb{H}$	*set of* Hours in one year
$\mathbb{L}$	*set of* Eligible location points
$\mathbb{C}$	*set of* Capacity factors

Calligraphic typefaces

$\mathcal{D}$	Virtual hydrogen demand, in kg
$\mathcal{F}$	Oversize factor, dimensionless

Greek symbols

Δ	Decommission value of the system, in EUR/kW
δ	Power degradation of the system, in percentage
υ	Annual utilisation factor, in kWh/kW
ρ	Production rate of the electrolyser, in kg/h/kW
η	All–round electric efficiency, in percentage

Roman symbols

$\mathtt{A}$	Area, in square meters
$\mathtt{CF}$	Capacity factor, in percentage
$\mathtt{D}$	Diameter, in meters
$\mathtt{GCR}$	Ground cover ratio, dimensionless
$\mathtt{I}$	Capital expenditure of the system, in EUR/kW
$\mathtt{i}$	Inflation rate, in percentage
$\mathtt{j}$	Replacement number, equal to 1 or 2
$\mathtt{K}$	Overall cost structure, in EUR
$\mathtt{L}$	Length, in meters
$\mathtt{LCOE}$	Levelised cost of electricity, in EUR/kWh
$\mathtt{LCOH}$	Levelised cost of hydrogen, in EUR/kg
$\mathtt{N}$	Economic lifetime of the system, in years
$\mathtt{n}$	Year number, ranging from 1 to N
$\mathtt{O}$	Annual operational expenditures, in EUR/kW/yr
$\mathtt{P}$	Nominal power, in watt
$\mathtt{r}$	Roughness length, in meters
$\mathtt{R}$	Electrolyser replacement cost, in EUR/kW
$\mathtt{RSD}$	Rotor safe distance, in meters
$\mathtt{S}$	Spread factor, dimensionless
$\mathtt{u}$	Wind speed, in m/s
$\mathtt{W}$	Width, in meters
$\mathtt{w}$	Weighted average cost of capital, in %
$\mathtt{Y}$	Global hydrogen yield, in kilograms
$\mathtt{z}$	Height, in meters
$\mathtt{Z}$	Virtual support variable, dimensionless

Subscripts

$\mathtt{0}$	*rel* Initial value
$\mathtt{ft}$	Offshore floating wind farms
$\mathtt{fx}$	Offshore fixed wind farms
$\mathtt{h}$	*rel* Hourly value
$\mathtt{H_2}$	*rel* Electrolyser
$\mathtt{K}$	*rel* Cost
$\mathtt{m}$	*rel* Solar module
$\mathtt{max}$	Maximum allowed
$\mathtt{nom}$	Nominal
$\mathtt{out}$	Output
$\mathtt{pv}$	Solar photovoltaic
$\mathtt{px}$	*rel* Pixel
$\mathtt{r}$	Real
$\mathtt{ref}$	Reference
$\mathtt{RES}$	Renewable energy source
$\mathtt{t}$	*rel* Turbine
$\mathtt{v}$	Virtual
$\mathtt{wd}$	Onshore wind
$\mathtt{Y}$	*rel* Yield

Superscripts

$\mathtt{(ft)}$	*rel* Offshore floating wind farms
$\mathtt{(fx)}$	*rel* Offshore fixed wind farms
$\mathtt{(pv)}$	*rel* Solar photovoltaic
$\mathtt{(wd)}$	*rel* Onshore wind farms
$\odot$	Optimal solution

systems to be out of the scope of this particular work—nonetheless, recognising such analysis to be of utmost importance for a comprehensive approach to the hydrogen industry. Even so, relying solely on occasional curtailed electricity to produce hydrogen implies electrolysers having very low utilisation factors (and, ultimately, very high unit costs). Hereupon emerges the relevant argument for extensive, dedicated hydrogen projects directly coupled with renewable energy sources. These systems can be located onshore or offshore, and have single or hybrid RES–to–Hydrogen configurations [4].

This work is then rooted in the central purpose of contributing to the study of these important issues, with a focus on two similar but distinct European countries to allow for a comparative analysis of hydrogen production potential. To put it another way, this research aims to determine which locations are suitable for installing renewable energy systems specifically designed to produce green hydrogen and what configuration yields the lowest cost of hydrogen production. To do that:

1. A map is made showing the locations that can be used to install renewable energy systems for the production of green hydrogen—these maps are limited to Italy and Portugal;
2. A ratio of the installed capacity of renewable energy sources to the nominal power of the electrolyser is calculated to be applied on large–scale, national systems;
3. An algorithm is created to determine the ideal sizes of electrolyser and renewable energy system pairs, taking into account both hybrid onshore and offshore configurations.

The *novel approach* is established, referring to the two models entirely developed from the ground up—a geographical model to identify the eligible locations and a numerical model to optimise RES-to-hydrogen system configurations. Point 1. offers an unprecedented accomplishment for these two nations in that they close a critical research gap related to the geographical assets of Italy and Portugal; such material data may be a valuable support to any economic analysis conducted by municipalities and even the central governments. Point 2. represents a significant improvement of the study's credibility, producing results ever closer to reality; this procedure constructively challenges the standard way of assessing large–scale green–hydrogen projects and thus may be replicated in subsequent analysis as a means to make estimations better resemble the real world. Point 3. grounds its foundation on a comprehensive problem setting and mathematical formulation, comprising the detailed definition of index sets, parameters, support and decision variables, as well as an objective function constrained by ten equations; when used on a country–specific set of points, the results validate the initial premise of the algorithm in providing the optimal computation of the levelised cost of hydrogen with notable success. A model with such attributes was yet to be found in the literature, evidencing its important contribution towards addressing this gap.

After this Introduction indicating the rationale and contributions of this work, the remainder of the document is organised as follows: Section 2 offers a comprehensive review of recent publications on the matters described so far and the identification of research gaps in the literature; Section 3 introduces the methods of investigation, elaborating on the different stages of designing the geographical model. Section 4 elaborates on the different stages of the numerical formulation that underlie the economic models while the results are presented an discussed Section 5 and Section 6, respectively. Finally, Section 7 provides the overall conclusions of the work.

2. Literature review

Nowadays, it is extraordinarily uncommon to study a subject completely unknown to the scientific community. On the contrary, most discoveries are increasingly achieved through joint efforts and supported by iterative research on the same matters. The topic of this study abides by that, so this section aims to present part of the body of knowledge published so far related to it—providing a broad overview of such issued works while addressing potential research gaps and the respective solutions hereafter hypothesised.

B. Franco [5] conducts a techno–economic analysis of hydrogen offloading systems for offshore wind farms. A major finding of this work is the improved economic viability of the projects when the market value of oxygen is considered (as a byproduct). A sensitivity analysis at the end also shows how the cost of hydrogen is mainly influenced by the costs of electricity and the electrolyser.

K. Narayan [6] instead focus on exploring hydrogen as a potential element to power long–distance, heavy–duty transport; the viability of switching different modes of transportation to green hydrogen is first addressed. A similar conclusion to the previous case is reached here, in the sense that selling the byproduct oxygen guarantees the economic viability of the projects. Furthermore, the sensitivity analysis also confirms that the cost of hydrogen mainly depends on capital costs and the cost of electricity.

C. Groenewegen [7] conducts a geospatial techno–economic analysis analogous to what is presented in this work. In it, the potential for large–scale, low–cost green hydrogen production is assessed in Europe and in the region of North–Africa. Considering it is based on rough, approximate models, this research still gives a good estimate of the potential for green hydrogen production.

Geographic information systems (GIS) have become a main tool around the world to use in the selection of the most fitting sites for the installation of RES–associated projects.

D. Vagiona and M. Kamilakis [8] present an integrated method to evaluate and prioritise suitable regions for developing sustainable offshore wind farms. The combined use of geographic information systems and multi–criteria decision methods outputs a result that ensures the spatial sustainability of the wind farms.

Juárez–Casildo et al. [9] explore the concept of hydrogen cities by proposing hydrogen production in urban settlements. Using GIS tools, the monthly potential of solar–hydrogen in metropolitan areas of Mexico is assessed. The authors conclude that the country's total annual hydrogen demand can be entirely satisfied by just one–month production of certain urban areas at a relatively low cost. Additionally, further conclusions agree with previous observations that metropolitan hydrogen production has low water requirements with a minimal infrastructure footprint.

B. Raillani et al. [10] aim to make a techno economic–evaluation of a large photovoltaic (PV) power plant dedicated to hydrogen production in eastern Morocco. A multivariate non–linear regression model is implemented to obtain a fitting energy production equation, adjusted to provide accurate, high–resolution GIS data.

Pandora G. S. and Theocharis T. [11] incorporate expert opinions and an extensive survey to local stakeholders into the GIS framework for optimal siting of offshore wind farms. Through several rigorous evaluation criteria, the study shows an over–potential capacity to cover the annual energy demand of Crete with just four wind farms.

T. Gunawan and his co–authors [12] develop a techno–economic model of distributed wind–to–hydrogen systems in Ireland. The systems are not completely off–grid since the grid may provide electricity when needed. Akin to a basic optimisation algorithm, the model uses a correlation–based approach to choose the optimal electrolyser capacity that yields the minimum LCOH, from a set of three scenarios. The conclusions coincide with the expected, in which the electrolysers must work at full capacity to reach a reasonably low LCOH.

Of the studies consulted, the majority consider the energy produced by the dedicated RES to be totally consumed by the electrolyser—implying that both systems are the same size. A more careful analysis instead looks at ways to optimise the size of the electrolyser, taking into account the electricity generated by renewable sources, to minimise project costs.

O. Atlam et al. [13] present one of the first methods to optimally size an electrolyser connected directly to a solar photovoltaic system. The method consists of a precise match of linear approximations of the electrolyser polarisation curve and the maximum power point curve of the PV system. The influence of PV temperature is also considered and found to be inversely correlated with the optimum size of the electrolyser.

More recently, the US National Renewable Energy Laboratory (NREL) published a comprehensive technical report on optimising integrated renewable electrolysis systems [14]. The study considers six different RES connections, including an 'islanded' one where no electricity purchases or sales are made to the grid. This configuration avoids market fees but limits the electrolyser to the solar capacity factor, resulting in initial higher unit costs.

Y. Jiang et al. [15] perform a size optimisation, techno–economic assessment of a far–offshore wind–to–hydrogen project. A chance–constrained programming model is built to establish a benchmark maximum net present value (NPV) of the project and information–gap decision theory is applied to check acceptable hydrogen price ranges. A particle swarm optimisation of stochastic simulation is selected to solve both models; in the end, a case study is used to demonstrate and compare results, including optimal size, economic viability and hydrogen prices.

M. Scolaro and N. Kittner [16] investigate the cost competitiveness of market ancillary services for offshore wind–based hydrogen production. The size of the electrolyser is determined through two different methods – optimal bidding strategy and optimal sizing of the facilities – and the project feasibility is evaluated by metrics such as the NPV and the LCOH. The authors conclude that these projects need participation in the ancillary service market to yield net positive revenues at present levels of wind generation.

Concerning LCOH optimisation, many different approaches exist depending on the desired outcome. Simple linear approximations may be a quick method but lack deep exactitude and generate low–value oversimplifications; particle swarm optimisation commonly requires fewer parameters and has easier constraints but may produce early convergence, low–quality solutions. Likewise, works like those discussed rarely include map–based optimal economical analysis of hydrogen systems. Also, few consulted papers provide an extensive, multi–criteria assessment of the available locations—and if they do, it is not broadly applied, e.g. to a whole country. In addition, neither of these articles presents a true LCOH mapping comprising the areas previously evaluated. Furthermore, no work has been found in the literature that simultaneously contains both onshore and offshore geographic analysis of the same region.

A collection of selected papers and their main takeaways is systematised in . With the research gaps identified, the solutions suggested throughout the material methods of this document intend to satisfy the objectives presented.

3. Geographical model design

This work focuses on two similar but distinct Mediterranean countries – in terms of solar exposure and wind profile, although recognising their clear differences, namely total onshore and offshore area and bathymetry outline – to enable a comparative examination of the potential for hydrogen production. Italy and Portugal were chosen as exemplary use cases since this analysis stems from an international collaboration bringing together researchers from both countries. Nevertheless, the developed model is location-agnostic and extensible to any other country, provided that the needed data is available.

This section presents the distinct stages of material work undertaken to design and develop the geographical model.

Identifying suitable locations for implementing solar parks and wind farms in a given geographic region involves several steps and compromises. Some related works [8,11,18] integrate multi–criteria decision–making methods to access the weight preferences and impacts of such compromises, namely through public surveys and expert interviews. Since such procedures were not conducted for this analysis, an equal–weight analysis is chosen.

The first stage of the methodology is collecting and analysing the geospatial data; the second consists of excluding incompatible areas according to selected criteria and surface area restrictions; these are defined considering a set of environmental, legislative, safety and technical constraints. The overlapping rejection of such constraints leads to the admissible areas, further evaluated in the third and last stage. This procedure is conducted on QGIS [19], the leading open–source desktop GIS software.

3.1. Data collection and analysis

A geographical framework begins with establishing its coordinate reference system (CRS). This process is required to avoid angular, length or area distortions on the imported data, enabling the precise algebraic computation of acceptable regions and the creation of buffer zones. The native geographic coordinate reference system of QGIS is the World Geodetic System 1984 (commonly referred to as WGS 84). Upon projection to the Universal Transverse Mercator (UTM) CRS, latitudes, longitudes and degrees are respectively converted to northing values, easting values, and distances. Since map projections never represent the exact sphericity of the Earth, the appropriate UTM zone should be used as CRS for each area of interest to minimise distortion and get correct analysis results. A summary of the aforementioned is presented in Table 2.

Once the coordinate reference system is set up, both raster and vector datasets are imported from a multitude of sources, summarised in Table 3. Raster files convey geospatial data as an image, with a specific extent and a pixel resolution; each of these pixels encompasses a unique value that defines a property of its respective location. Vector datasets, on the other hand, supply information as a compilation of features and their related attributes; each feature is given by a geometry that may be a point, a line, or a polygon.

These create a work structure on which additional datasets are superimposed, enabling the exclusion and evaluation phases of the methodology. For simplicity's sake, yet without compromising the accuracy of results, a general resolution was defined as 1 km^2. Higher resolutions were found to bring no benefit to country–scale analysis; furthermore, some of the raster files also do not have higher resolutions, thus eventually leading to wasted computational effort if a more refined mesh was chosen. Correcting some geometries before applying further processing is often needed, as well as creating spatial indexes that increase the performance of the operations. After these procedures, every exclusion criterion is categorised into its respective group, and an appropriate buffer is applied, following the method described next.

3.2. Data exclusion

This operation starts with setting a buffer over the constraints previously categorised into four main restriction criteria—environmental, legislative, safety and technical, a distribution that follows the ones found in literature [31,32].

Any *environmental criterion* is generally characterised by zones of recognised natural and ecological value and beauty, where the viability and conservation of biodiversity are ensured through legislation. Onshore locations have buffers of up to 1000 meters [32], while offshore sites have none [11,33,34].

A *legislative criterion* is provided by law and intends to define acceptable regions through a safe distance from terrestrial and maritime infrastructure. This analysis divides terrestrial infrastructure into 'Transport Facilities' and 'General Buildings', while offshore locations include the safe distance to 'Fishing Areas', 'Island Settlements' and more broadly, the 'Shore'. These buffers range from 500 to 5000 meters [11,32,35].

Safety criteria encompass those related to the safe operation of transport activities, whether on land (rail or road), air or sea—'Railways', 'Major Roads', 'Airports' and 'Shipping Routes'. Buffers of these locations go from 50 meters onshore to 3000 meters offshore [11,32,36].

Table 1
Summary of literature review articles and their main methods.

	Ref.	Author	Journal	Main methods
Geospatial–based techno–economic analysis	[8]	D. Vagiona and M. Kamilakis (2018)	Sustainability	Integrated method for evaluation and prioritisation of suitable regions; combined use of geographic information and multi-criteria decision methods.
	[9]	Juárez-Casildo et al. (2022)	International Journal of Hydrogen Energy	Metropolitan production of hydrogen may satisfy the needs of the country at relatively low cost and require less water and a minimal footprint.
	[10]	B. Raillani et al. (2022)	Energy for Sustainable Development	Multivariate non–linear regression model to obtain energy production equations and adjusted to provide accurate GIS data.
	[11]	Pandora G. S. and Theocharis T. (2022)	Energy	Perform extensive surveys to local stakeholders and gather expert opinions to incorporate into the GIS framework for optimal siting of offshore farms.
	[17]	T. Gunawan et al. (2020)	Energies	Correlation–based approach to get the electrolyser capacity yielding the minimum LCOH in a distributed wind–to–hydrogen system.
	[7]	C. Groenewegen (2021)	TU Delft	Geospatial techno–economic analysis of the potential for large–scale, low–cost hydrogen production in Europe and the North of Africa.
Optimal computation of hydrogen costs	[13]	O. Atlam et al. (2011)	International Journal of Hydrogen Energy	Optimally size an electrolyser connected to a solar PV farm and precisely match linear approximations of the electrolyser polarisation curve.
	[15]	Y. Jiang et al. (2022)	International Journal of Hydrogen Energy	Perform a techno–economic assessment using a chance–constrained programming model built to establish a benchmark maximum NPV.
	[16]	M. Scolaro and N. Kittner (2022)	International Journal of Hydrogen Energy	Investigate the cost competitiveness of market ancillary services through optimal bidding strategies and optimal sizing of the facilities.
	[5]	B. Franco et al. (2021)	Applied Energy	Techno–economic analysis of hydrogen offloading systems for offshore wind farms, considering the selling of oxygen as byproduct.
	[6]	K. Narayan et al. (2021)	UL–IST	Focus on exploring hydrogen as a potential element to power long–distance, heavy–duty transport.

Table 2
Coordinate reference system of each study area.

Study area	Geodetic CRS	Projected CRS	Public registry	Ref.
Italy	WGS 84	UTM zone 32N	EPSG:32632	[20]
Portugal	WGS 84	UTM zone 29N	EPSG:32629	[21]

Finally, a *technical criterion* regards fixed infrastructure already deployed in a potentially admissible area. For instance, 'Pipelines', 'Powerlines' and submarine energy interconnections. Most of these categories imply a 100–meters buffer, with offshore sets up to 500 meters [32,37–39].

3.3. Data evaluation

Following the creation of acceptable areas through data exclusion, the last step of the methodology consists of their evaluation through characteristic criteria. These parameters concern region–specific physical attributes, on which limits are imposed to maximise energy production.

Mean elevation is included in this analysis on the premise that RES suitability decreases at extreme altitudes, mainly due to diminishing resources (like lower air density or increased cloud coverage) and increased inaccessibility, leading to higher installation costs. The exclusion threshold is set to 2000 m, following the literature review by D. Rayberg [32]. Since the highest peak in continental Portugal is only 1993 m, no elevation restrictions exist there.

The *average terrain slope* is an essential physical criterion in pair with elevation; in this work, it is used to evaluate the terrain's angle and orientation. Slopes not facing between southwest and southeast can be excluded from photovoltaic siting analysis, although that not being the case here. Most studies in the literature [32] typically set a threshold on average terrain slopes above 10° since steeper topographies are found to cause problematic installation of solar panels and wind turbines. Note that this attribute should not be confused with the tilt of the solar modules; generally, fixed panels are installed with a tilt angle approximately equal to the latitude of the place where they are located—a simple, cheap method but not the most efficient.

It is a well–known phenomenon that increasing *air temperature* leads to a decrease of the photovoltaic module's voltage output. Several simplified relations exist that linearly correlate the module's temperature with air temperature, solar irradiance and the normal operating cell temperature of the module; the panels used in this work require air temperatures between −10 °C and 50 °C for regular operation.

Besides, warmer air is less dense than cold air, so in hotter locations, there is a decrease in the turbine's electric yield since there is a lower energy extraction from the wind. Consequently, in this analysis, cooler air is always preferred for renewable electricity generation.

Bathymetry describes depth variations in the ocean's seabed (analogous to submarine orography). Water depth is a crucial criterion for assessing the siting of offshore wind farms since, typically, these require less than 50 meters of water depth for fixed foundation turbines. On the other hand, floating wind technologies are currently estimated to be economically feasible for water depth down to 1000 m, mainly due to the mooring, anchorage and cabling works used. This analysis follows the recommendation of Global Wind Atlas [40], which also corroborates most of the published studies consulted in the literature [8,11,31].

Mean wind speed is one of the primary ways to measure wind energy resources. In general, the wind velocity profile in the atmosphere increases with height, which is why turbines have steadily become taller and taller over the years. At greater heights, the wind velocity profile in the atmosphere increases—but it is also where the air is less dense, which causes diminishing energy resources (since the power of a wind–stream is directly proportional to air density). However, it varies to the cube of wind velocity, so essentially, higher wind speeds correspond to higher energy availability.

Average wind speeds are commonly measured from meteorological observations at 10 meters above ground level and then converted to the desired rotor height. Turbine manufacturers determine cut–in and

Table 3
Data collection: source and format of the data layers.

Source	Data layer	Format	Source	Data layer	Format
[22]	Countries in Europe	Polygon vector	[23]	Boundary of Italy	Polygon vector
[24]	Europe hillshade	DEM[a] raster	[25]	Italy regions	
[26]	Countries in Africa	Polygon vector	[27]	Italy EEZ	
[24]	North–Africa hillshade	DEM raster	[28]	Boundary of Portugal	
[29]	Mediterranean Sea	Polygon vector	[25]	Portugal regions	
[30]	Mediterranean bathymetry	DEM raster	[27]	Portugal EEZ	

[a] Digital elevation model.

Table 4
Summary of the results for eligible locations.

	Total area (km^2)		Available area (km^2)		Fraction (%)	
	Onshore	Offshore	Onshore	Offshore	Onshore	Offshore
Italy	300 979	536 654	37 637	104 338	12.50	19.44
Portugal	89 015	315 598	24 734	22 495	27.79	7.13

cut–out speeds at those heights to protect the turbine from damage, usually fixating them between 3 m/s and 25 m/s [41]. These limits are also applied in this analysis.

3.4. Eligible locations

Once the evaluation and exclusion criteria have been established, the corresponding restricted zones are combined to form a layer described as "incompatible locations". These locations reflect the current areas in each country where installing a RES system for producing green hydrogen is not feasible because the land is buffered (per the guidelines used in the previous sections) or is already occupied by other socioeconomic activities. The "eligible locations" data layer is then created by geometrically subtracting these polygons from the country's entire surface. These, as opposed to the earlier ones, are suitable places to develop green hydrogen projects today. The information mentioned above is shown in Fig. 1, which shows both countries as either *eligible* (in blue) or *incompatible* (in red) locations.

To better assess the visual results of these maps, the available area and the respective percentage fraction of the total area (onshore and offshore) of both countries are computed and displayed in Table 4.

As expected, most of the total area in Italy and Portugal is already occupied. In the case of Italy, most of the areas eligible for offshore wind are in the South, mainly surrounding the two main islands of Sardinia and Sicily. Onshore, the northern part is almost empty of eligible locations since it is more urbanised than the southern areas. Moreover, Italy has the Alps in the north and the Appennine from north to south, where installing RES is not easy. With Portugal, the situation is similar; the great urbanised regions on the coast have the least eligible locations, while the interior centre and north have the most availability. Offshore, most of the blue zones are below Lisbon in the western and southern parts of the Atlantic.

Even so, in any case of country–wide analysis, small fractions of available land may correspond to large surface areas in absolute terms—which is the case here. The regions available for installing renewable energy projects have a massive potential to shift the energy mix of both countries.

Each of the points yielded by the geographic model is a potential eligible location for the installation of a green hydrogen project, whose economic viability is assessed in the following section.

4. Numerical model layout

Every economic assessment requires the development of a numerical model that computes the outcome predictions from the input data. This section describes the development of the two numerical models used in this economic analysis. Section 4.1 first addresses the calculation of both the levelised cost of hydrogen and the levelised cost of electricity (LCOE)—a sub–component of the former—for each renewable energy source considered: solar photovoltaic parks, onshore wind farms, and offshore fixed/floating wind farms. Section 4.2 then takes these calculations and employs them into a generalised model to be applied to the whole set of locations of both countries. Finally, Section 4.3 improves on the generalised model and describes the development of a specific optimisation model.

4.1. Hydrogen economic fairways

In this work, the pathway to define the economic viability of the hydrogen projects is based on the method recently employed by S. Walsh et al. [42]. He and his team performed a study using the Bluecap software and the Hydrogen Economic Fairways Tool, hosted on Geoscience Australia's portal [43]. Likewise, this analysis applies a sub–model developed in Microsoft Excel, which considers all the distinct parameters essential to compute the cost of hydrogen production in the eligible locations obtained in the previous chapter.

The following subsection delves into the specifics of calculating the LCOH, depending on the RES associated with the project; however, there are two general and independent parameters, which are the same for the four calculations: the project lifetime and the inflation rate.

The lifetime of these projects is assumed to be 30 years. This choice reflects the IEA PVPS Task 12 recommendation for life cycle assessment studies and matches the quality of current solar photovoltaic systems [44]. Wind turbine projects have traditionally shorter technical lifetimes (around 20 years). However, since more and more studies are presently looking at turbine life span extension strategies [45,46], the applied system lifetime is the same. In any case, the operational period of RES projects is expected to increase henceforth [44].

Inflation rates in Europe have changed dramatically during the past decades, reaching an all–time high of 8.90% in July 2022 [47]. Nevertheless, following E. Vartiainen et al. [44], an inflation rate of 2% is considered the recent historical average of the Eurozone—and thus is used in this analysis. This premise directly impacts the difference between the nominal and real weighted average cost of capital (WACC). Most projects use this metric as a proxy for the discount rate since it refers to the required return rate to make an investment worthwhile. This work only distinguishes between nominal and real WACC: the former accounts for inflation, and the latter does not. Eq. (1) shows the Fisher equation, with which these values can be computed (following Bjarne Steffen's [48] method).

$$1 + \mathtt{w}_{\mathtt{nom}} = (1 + \mathtt{w})(1 + \mathtt{i}) \tag{1}$$

where:

$\mathtt{w}_{\mathtt{nom}}$ is the nominal WACC.
$\mathtt{w}$ is the real WACC.
$\mathtt{i}$ is the inflation rate.

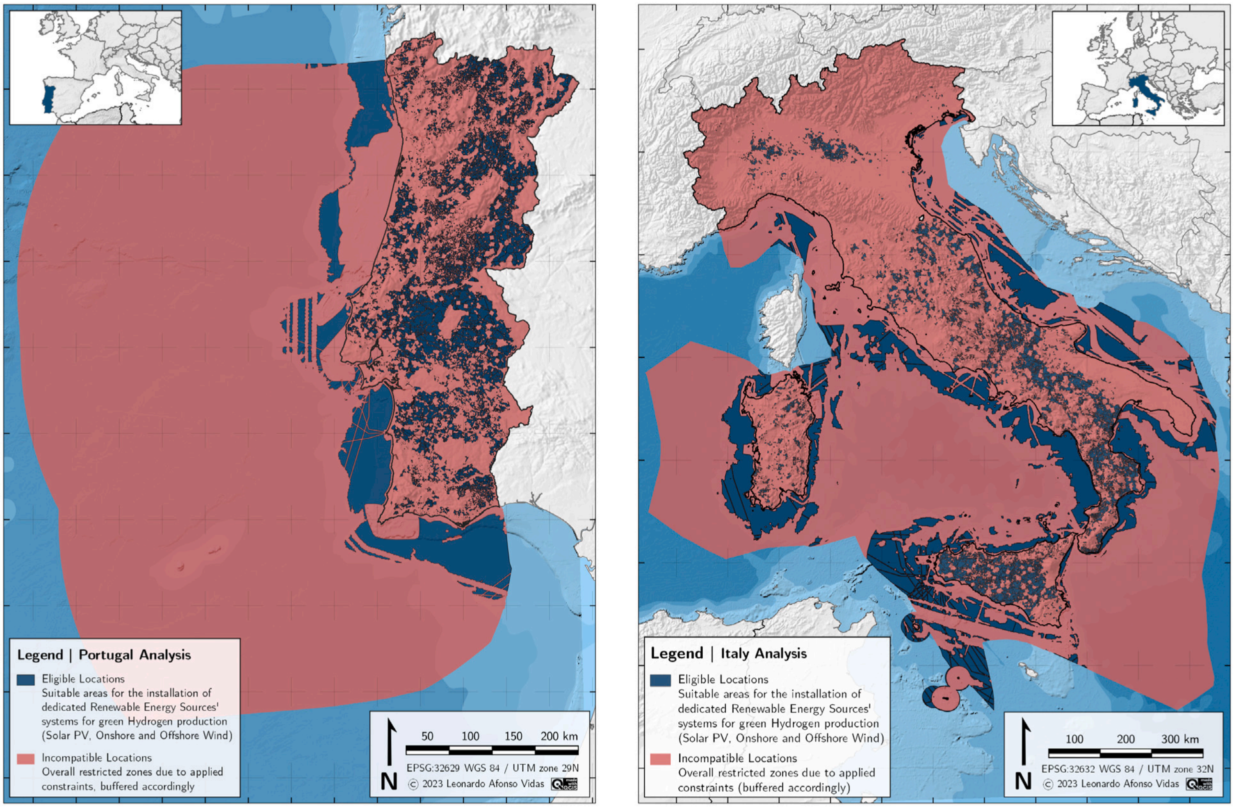

(a) Portugal   (b) Italy

Fig. 1. Country analysis: total eligible locations.

4.1.1. *Levelised cost of hydrogen*

The levelised cost of hydrogen is a benchmark commonly used to determine the feasibility of a hydrogen project. Above all, it measures the cost of producing one hydrogen unit during the project's lifetime. Eq. (2) presents the generalised formulation used in this analysis.

$$\mathtt{LCOH}^{(*)} = \frac{\mathtt{K}_{\mathtt{RES}} + \mathtt{K}_{\mathtt{H}_2}}{\mathtt{Y}_{\mathtt{H}_2}} \tag{2}$$

Note: $^{(*)}$ is replaced according to the RES associated with the calculation: **(pv)** for solar photovoltaic parks, **(wd)** for onshore wind farms, **(fx)** for offshore fixed wind farms or **(ft)** for offshore floating wind farms.

where:

- $\mathtt{K}_{\mathtt{RES}}$ is the overall cost structure of the RES power plant, in EUR.
- $\mathtt{K}_{\mathtt{H}_2}$ is the overall cost structure of the electrolyser, in EUR.
- $\mathtt{Y}_{\mathtt{H}_2}$ is the global hydrogen yield, in kg.

The generalised formulation has many sub–components aggregated into progressively broader concepts. These concepts are explored in the following equations, based on the works of M. Minutillo et al. [49], L. Viktorsson et al. [50] and T. A. Gunawan et al. [17]. Eq. (3) develops the formulation of $\mathtt{K}_{\mathtt{RES}}$.

$$\mathtt{K}_{\mathtt{RES}} = \left[\mathtt{I}_0 + \sum_{\mathtt{n}=1}^{\mathtt{N}}\left(\frac{\mathtt{O}_{\mathtt{K}}}{(1+\mathtt{w}_{\mathtt{nom}})^{\mathtt{n}}}\right) - \frac{\Delta_{\mathtt{N}}}{(1+\mathtt{w}_{\mathtt{nom}})^{\mathtt{N}}}\right]_{\mathtt{RES}} \times \mathtt{P}_{\mathtt{RES}} \tag{3}$$

where:

- $\mathtt{N}$ is the economic lifetime of the system, in years (assumed to be 30).
- $\mathtt{n}$ is the year number, ranging from $\mathtt{1}$ to $\mathtt{N}$.
- $\mathtt{I}_0$ is the total capital expenditure of the system, made at $\mathtt{n} = 0$, in EUR/kW.
- $\mathtt{O}_{\mathtt{K}}$ is the total all–in expected operational cost of the system, at any given year, in EUR/kW/yr.
- $\Delta_{\mathtt{N}}$ is the decommissioning value of the system, at year N, in EUR/kW (assumed to be zero).
- $\mathtt{w}_{\mathtt{nom}}$ is the nominal WACC, in percentage.
- $\mathtt{P}_{\mathtt{RES}}$ is the installed capacity of the RES power plant, in kW.

The decommission value of the system at the end of the project's life includes the decommission expenditures (DecEx) and the end–of–life salvage value of the components. Since there is still no agreed price for such elements [44], this value is here defined as zero: $\Delta_{\mathrm{N}} = 0$. Nevertheless, this parcel is still relevant to add to the equation because typically, the residual value of a dismantled PV/wind system is positive [51,52]—and so, if there is any inaccuracy in this formulation, is of an overestimation error, not underestimation (i.e. the final LCOH may be even lower than what is presented).

The total CapEx of the RES system is assumed to be paid in full before the project begins operation, thus not needing to be discounted to the present.

Each system's total all–in operational expenditure consists of both operations and management and services costs (scheduled and unscheduled) and other expenses. It is a fixed annuity.

The constant value of O_{K} leaves the summation since it is a series of equal annual payments that need to be discounted to the present value; the remaining term is thus expressed as an elementary finite geometric series. The *capital spread factor* is so defined as the inverse of the well–known *capital recovery factor*, and can be found using Eq. (4).

$$\sum_{\mathtt{n}=1}^{\mathtt{N}} \frac{1}{(1+\mathtt{w}_{\mathtt{nom}})^{\mathtt{n}}} = \frac{(1+\mathtt{w}_{\mathtt{nom}})^{\mathtt{N}} - 1}{\mathtt{w}_{\mathtt{nom}} \times (1+\mathtt{w}_{\mathtt{nom}})^{\mathtt{N}}} \equiv \mathtt{S}_{\mathtt{K}} \tag{4}$$

This factor is used in the following subsections as a multiplication element to discount sets of equal annual amounts systematically. Eq. (5)

Table 5
Summary of the LCOH components for every RES formulation.

		Unit	Solar photovoltaic	Onshore wind	Offshore fixed	Offshore floating	PEM electrolyser
General parameters							
N	Operational lifetime	years			30		
i	Inflation value	%			2		
Economic factors							
w_{nom}	Nominal WACC	%	5.40	7.30	8.30	8.30	n/a
w	Real WACC	%	3.33	5.20	6.18	6.18	n/a
I_0	Capital expenditures	EUR/kW	630	1162.48	1703.63	3604.63	1136.20
O_K	Operational costs	EUR/kW/yr	10.89	37.04	61.02	65.45	14.97/34.09
R	Replacement cost	EUR/kW		n/a			681.72
Δ_N	Decommission value	EUR/kW			0		
Technical aspects							
δ_n	Degradation value	%/year	0.45	0.39	0.39	0.39	0.70
ρ	Production rate	kg/h/kW			n/a		0,01771
η	System efficiency	%			n/a		60

now further expands the components of K_{H_2} formulation.

$$K_{H_2} = \left[I_0 + \sum_{n=1}^{N} \left(\frac{O_K}{(1+w_{nom})^n} \right) + \sum_{j=1}^{2} \left(\frac{R_{jN/3}}{(1+w_{nom})^{jN/3}} \right) - \frac{\Delta_N}{(1+w_{nom})^N} \right]_{H_2} \times P_{H_2} \tag{5}$$

where:

N is the economic lifetime of the system, in years (assumed to be 30).
n is the year number, ranging from 1 to N.
I_0 is the total capital expenditure of the system, made at $n = 0$, in EUR/kW.
O_K is the total all–in operational expenditure of the system, in EUR/kW/yr.
j is the replacement number, with $j = 1, 2$.
$R_{jN/3}$ is the electrolyser replacement cost, happening at years 10 and 20, in EUR/kW.
Δ_N is the decommission value of the system, at year N, in EUR/kW (assumed to be zero).
w_{nom} is the nominal WACC, in percentage.
P_{H_2} is the electrolyser rated power, in kW.

The electrolyser, all necessary balance of system (BOS) costs, and soft costs are included in the system's total capital expenditure. Like its RES equivalent, it does not need to be discounted because it is assumed to be paid in full before the project starts.

Once more, both fixed and variable operations and management costs make up the entire all–in operational expenditure. Thus, O_n is likewise a fixed annuity discounted to the present value with the previously computed S_K factor.

As per the most recent DBEIS report [53], replacement expenses (ReplEx) for PEM electrolysers are estimated to be approximately 60% of the initial capital expenditure (CapEx) and are presumed to be required every 11 years during a technical lifetime of 30 years. Instead, two 10–year replacement periods are assumed for the purposes of this analysis.

For consistency's sake, the decommissioning value of this system is taken to be zero, just like in the prior instance.

After describing the two components of the numerator, the denominator component is the only thing left to discuss. The global hydrogen yield formulation is then shown in Eq. (6).

With both parts from the numerator explained, it remains only to describe the denominator component. Eq. (6) then presents the formulation for the global hydrogen yield.

$$Y_{H_2} = \sum_{n=1}^{N} \left(\frac{\upsilon \times P_{RES} \times (1-\delta_{RES})^n}{(1+w)^n} \times \frac{\eta \times \rho \times (1-\delta_{H_2})^n}{P_{H_2}} \right) \tag{6}$$

where:

N is the economic lifetime of the system, in years (assumed to be 30).
n is the year number, ranging from 1 to N.
υ is the annual utilisation factor of the power plant (full load hours), in kWh/kW.
P_{RES} is the installed capacity of the RES power plant, in kW.
δ_{RES} is the annual power degradation of the RES system, in percentage.
η is the all–round efficiency of the system, from the RES output to the stack input, in percentage.
ρ is the net production rate of the electrolyser, in kg/h.
δ_{H_2} is the annual power degradation of the electrolyser, in percentage.
P_{H_2} is the electrolyser rated power, in kW.
w is the real WACC, in percentage.

A power plant's full load hours (FLH) is typically used to indicate its annual utilisation factor [54]. This idea is expanded to electrolysers since the quantity of FLHs they require depends on the type of electricity that supplies them. For RES–to–Hydrogen projects such as the ones in this work, FLHs are heavily reliant on the location and availability of renewable resources.

In order to provide the most accurate findings possible, degradation rates are included; Table 5 displays these numbers, which vary based on the RES technology.

Based on the most recent public report from Gigastack [55], a figure of 0.08% per 1000 h is selected for the electrolyser's yearly power degradation. This term is changed to an annual rate to be consistent with the other deterioration rates in the model, as follows: $0.08 \times 8760/1000 = 0.7008\%$.

A number of currently available examples are used to determine the efficiency of the system and the net production rate of the electrolyser: the M Series from NEL [56], the HyLYZER system from Cummins [57], PlugPower [58]'s GenFuel ecosystem, and Siemens Energy's Silyzer [59]. The selected features are based on the ones that have the most information available, as none of these have a comprehensive technical datasheet. From this group, production rates typically approach 425 kg/day per MW–installed, which leads to $\rho = 0.01771$ kg/h per kilowatt–installed. The all–round efficiency is set to 60%, supported by the preeminent report of the IEA [3].

The production of hydrogen is discounted to its present value, just like the previously discussed instance of discounted expenses. Except for the degradation rates, note that all aforestated variables are independent of the year number. Thus, when the capital spread factor is calculated using a similar logic, all constants are eliminated from the summation, and the remaining term is represented by a finite geometric

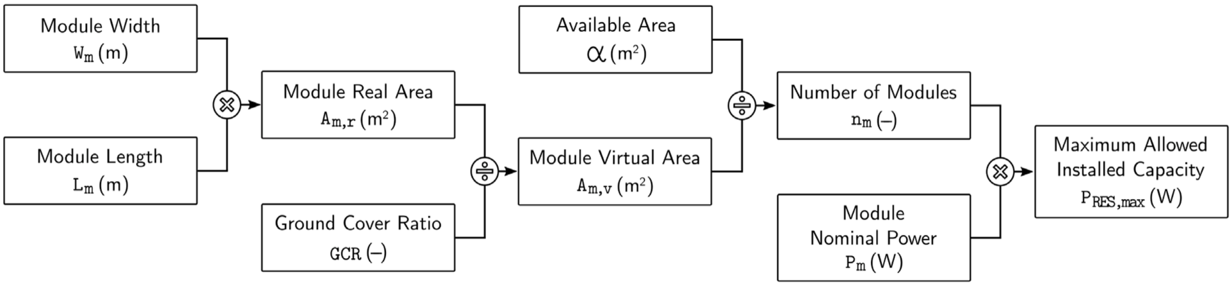

Fig. 2. Installed capacity upper–limit flowchart for photovoltaic solar parks.

series. The formula for the yield spread factor can be found in Eq. (4).

$$\sum_{n=1}^{N} \frac{(1-\delta_{RES})^n \times (1-\delta_{H_2})^n}{(1+w)^n} = \frac{(\delta_{RES}-1)(\delta_{H_2}-1)(1+w)^N \left[(1-\delta_{RES})^N(1-\delta_{H_2})^N-(1+w)^N\right]}{\delta_{RES}\times\delta_{H_2}-\delta_{RES}-\delta_{H_2}-w} \equiv S_Y \tag{7}$$

With the general formulation of the levelised cost of hydrogen fully defined, a specific equation can be found for every RES technology. Table 5 provides a summary of the variables considered. Please note that the two values presented for operational costs of the PEM electrolyser refer to onshore and offshore locations, respectively.

4.1.2. Levelised cost of electricity

While the central purpose of this work is to study the levelised cost of hydrogen, the computation of the levelised cost of electricity in energy systems is typically regarded as a valuable asset.

The LCOE is a metric usually associated with the feasibility of an energy project, measuring the cost of production of one energy unit during the lifetime of that project.

Eq. (8) shows the general formula used in this analysis.

$$LCOE^{(*)} = \frac{K_{RES}}{Y_{RES}} \tag{8}$$

where:

K_{RES} is the overall cost structure of the RES power plant, in EUR.
Y_{RES} is the total electricity generation, in kWh.

This formula resembles Eq. (2)—where the levelised cost of hydrogen is presented—, only here there is no cost associated with the electrolyser system, and the yield is electricity instead of hydrogen. K_{RES} is defined precisely like in Eq. (3) and respects all the assumptions made before for each one of the four technologies. Y_{RES} comes from the same formulation as in Eq. (6), neglecting the terms related to the electrolyser system. Eq. (9) displays the expanded form of the LCOE.

$$LCOE^{(*)} = \frac{I_0 + O_K \times \sum_{n=1}^{N} \frac{1}{(1+w_{nom})^n}}{\upsilon \times \sum_{n=1}^{N} \left(\frac{1-\delta_{RES}}{1+w}\right)^n} = \frac{I_0 + O_K \times S_K}{\upsilon \times S_Y} \tag{9}$$

with:

$$S_K = \frac{(1+w_{nom})^N - 1}{w_{nom} \times (1+w_{nom})^N} \quad \bigwedge \quad S_Y = \frac{(1-\delta_{RES}) \times \left[1 - \left(\frac{1-\delta_{RES}}{1+w}\right)^N\right]}{\delta_{RES} \times w}$$

Note that while the capital spread factor is identical to the one computed in Eq. (4), the yield spread factor here is simplified (due to the nonexistence of the electrolyser degradation rate).

This formula will be used as before to calculate the LCOE value of each RES technology for each location.

With the description of these formulations complete, the following section outlines the methodology associated with the simplified model of computing the levelised cost of hydrogen in Portugal and Italy.

4.2. Simplified general model

Many articles have been published in the literature where a geographic analysis of the LCOH is carried out, from individual countries such as Mexico [9], Morocco [10] and Ireland [12] to whole continents like Europe [7]. In all of these, the global hydrogen yield is assumed to be converted directly from the electricity generated by the renewable energy source, usually using the net production rate of the electrolyser or the lower/higher heating value of hydrogen.

Despite being extremely effective, this method lacks the inherent complexity of a real RES–to–Hydrogen system, a topic further addressed in Section 4.3. Even so, a similar model to those used in the literature is developed here to implement on all eligible locations of both countries. This section describes the creation of the simplified general model (SGM), starting by explaining how to determine the upper–limit of the RES installed capacity for a given available area and then discussing the definition of the localised LCOH computation.

4.2.1. RES maximum allowed capacity

As will be seen in the next subsection, the calculation of the levelised cost of hydrogen starts from the setting of a virtual hydrogen demand, from which the size of the RES capacity is estimated. Still, initially, it is imperative to establish the theoretical maximum limit based on the physical constraint of the available area.

For this, a flowchart illustrates the thought process behind the decisions made for both solar panels and wind turbines. Fig. 2 shows the flowchart to compute the maximum allowed solar installed capacity.

A generic utility–scale module is chosen [60], and the computations made according to the previous flowchart. The ground cover ratio (GCR) value follows the recommendation of T. Mahachi and A. Rix [61], in which the standard industry practice to optimise land–use on photovoltaic parks considers a 2.5% shading loss (shading derate factor of 0.975). In an effort to match the tilt angle of the panels to the average latitude of both countries, a value of 40° is selected; with the specific data of this analysis, GCR = 0.42.

The choice of the total available area per pixel (α) refers to a common spatial resolution in geographical models—1 km^2. An adjustment is made to accommodate the electrolyser and all balance of system footprint, leaving a space of 780 by 780 meters free for the RES installed capacity.

Table 6 outlines the value structure of the decision process described so far.

Fig. 3 now shows the equivalent decision flowchart for wind turbine farms.

The International Electrotechnical Commission Class II [62] is used as reference for the turbine features: 3.45 MW rated power, a diameter of 126 meters and a hub height of 100 meters. Nowadays, most sources [63–65] agree on placing onshore turbines seven rotor

Table 6
Summary of components in the computation of the maximum allowed solar installed capacity.

	W_m (m)	L_m (m)	$A_{m,r}$ (m^2)	GCR (–)	$A_{m,v}$ (m^2)	W_{px} (m)	L_{px} (m)	α (m^2)	n_m (–)	P_m (W)	$P_{RES,max}$ (MW)
Solar Photovoltaic	1.30	2.17	2.83	0.39	7.26	780	780	608400	83840	600	**50.30**

Note: coloured cells indicate values derived from the formulas described before.

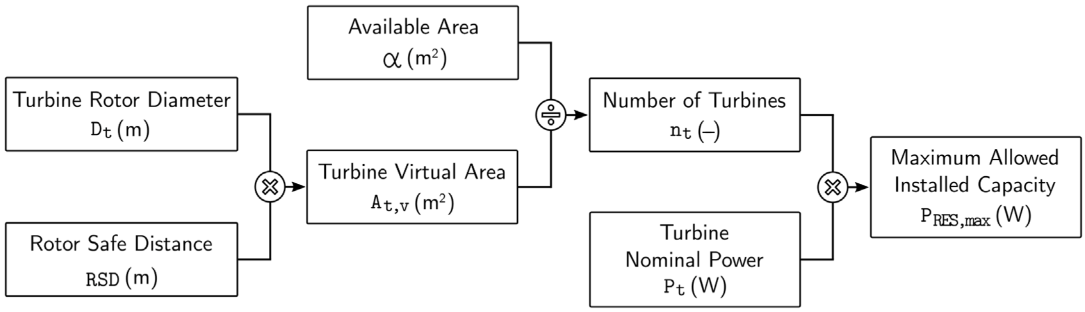

Fig. 3. Installed capacity upper–limit flowchart for wind farms.

Table 7
Summary of components in the computation of the maximum allowed wind installed capacity.

	D_t (m)	RSF (–)	RSF (–)	RSF (m)	$A_{t,v}$ (m^2)	W_{px} (m)	L_{px} (m)	α (m^2)	n_t (–)	P_t (MW)	$P_{RES,max}$ (MW)
Onshore Wind	126	7	5	35	4410	780	780	608400	138	3.45	**475.96**
Offshore Fixed	126	8	8	64	8064	780	780	608400	75	7.00	**528.13**
Offshore Floating	126	8	8	64	8064	780	780	608400	75	7.00	**528.13**

Note: coloured cells indicate values derived from the formulas described before.

diameters away from each other downwind and five rotor diameters sidewind. Regarding offshore farms, both these numbers increase to eight since turbines spaced further apart have been found to improve their efficiency and lifetime [63]; besides, covering a larger area is less of a problem on the sea.

The subsequent procedure is the same as for the solar parks; the total available area is also one pixel with approximately 1 km^2. Table 7 presents the values of each component in the decision process described before for onshore, offshore fixed and offshore floating wind farms.

With the installed capacity limit of every RES defined, the following subsection explores the reasoning behind structuring the simplified general model.

4.2.2. Localised LCOH computation

As explained in the preceding sections, this work starts by employing a generalised LCOH model. With the fundamental parameters of the electrolyser identified (ρ, η), the SGM starts from the definition of a virtual hydrogen demand, $\mathcal{D}$. This value represents a broad hydrogen need to be fulfilled in the regions where the project's economic feasibility is being evaluated; here, is defined as 10 kton/year. Next, from this hydrogen demand, the amount of electricity needed at the stack input is computed using the net production rate of the electrolyser. When the electrolyser system's electric efficiency is considered, one gets the yearly energy needed to be generated by the coupled RES power plant. Finally, to find the size of the RES station, a division is made of this quantity by the full load hours of the power plant. The annual solar and wind capacity factors are respectively collected from Global Solar Atlas [66,67] and Global Wind Atlas [68,69]. After proper data management in QGIS, a list of all capacity factors is converted to FLH and stored in each set $C^{(*)}$.

The size of the RES power plant is then tested against the upper–limits computed before to comply with the maximum physical allowance of installed capacity. If it is above the upper–limit, then the virtual hydrogen demand is adjusted for that particular location; if it is below, then it is clear to proceed.

The next step is the sizing of the electrolyser. Most of the consulted literature [7,9,10,12] just considers the electrolyser to have the same size as the RES station—this represents an oversimplified solution. Fig. 4 illustrates the energy production profile from solar PV (yellow) and onshore wind turbines (blue) during a typical day. The cited articles presume that the rated power of the electrolyser (green) coincides with the nominal installed capacity of the RES power plants, as shown (assuming nominal power is reached during the day).

Note that every region bounded by the green and yellow/blue lines reveals a period when the stack is not entirely in use. This setup inherently drives to waste most of the power from the electrolyser—in this example, around 27% if connected to onshore wind turbines, and up to 58% if connected to solar PV. In other words, this configuration leads to a lower electrolyser capacity factor and, in turn, increased relative costs.

For this reason, in this work, an oversize factor ($\mathcal{F}$) is applied instead: a ratio to apply between P_{RES} and P_{H_2} that best optimises the hydrogen output. The method to obtain this factor is described in the next subsection.

With the size of both the RES power plant and the electrolyser defined, Eq. (2) is used to find the respective LCOH. An additional procedure is required in onshore locations to evaluate which technologies yield the lowest cost since only one can be installed; after a direct comparison, the cheapest LCOH is selected for that location.

Algorithm 1 offers a pseudo-code summary of the process supporting the simplified general model tabulated form.

4.3. Optimised general model

With the disadvantages of the simplified method identified, the need to develop an optimisation algorithm is evident.

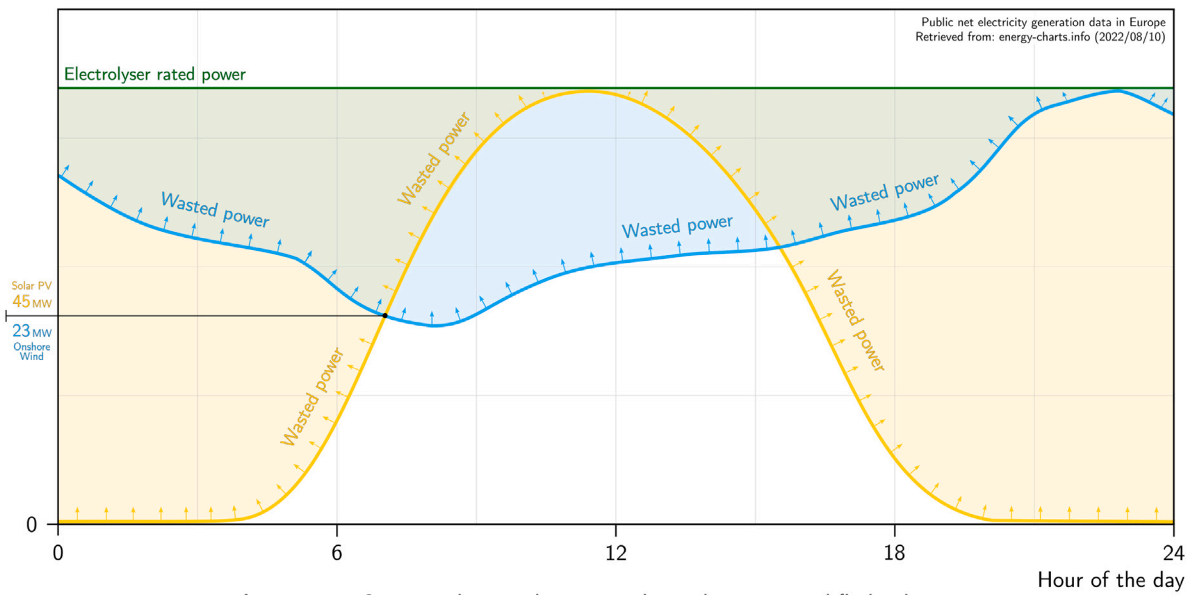

Fig. 4. RES–to–Hydrogen direct coupling: the oversimplified solution.

Algorithm 1 Simplified General Model algorithm

Require: $\mathcal{D}$, ρ, η, υ ▷ Parameters of the model
procedure SGM($\hookleftarrow$)
  for all $\upsilon \in \mathbb{C}^{(*)}$ **do**
    $\mathcal{D} \leftarrow$ ▷ Set hydrogen virtual demand
    $\mathcal{D} : \rho : \eta : \upsilon = \mathrm{P_{RES}}$ ▷ Compute power plant size
    if $\mathrm{P_{RES}} > \mathrm{P_{RES,max}}$ **then**
      decrease $\mathcal{D}$
    else
      $\mathcal{F} \leftarrow$ ▷ Set oversize factor
      $\mathrm{P_{RES}} : \mathcal{F} = \mathrm{P_{H_2}}$ ▷ Compute electrolyser size
    end if
    procedure Onshore LCOH$^{(*)}$
      if LCOH$^{(pv)}$ **then**
        use Eq. (2)$^{(pv)}$
      else if LCOH$^{(wd)}$ **then**
        use Eq. (2)$^{(wd)}$
      end if
      if LCOH$^{(pv)}$ < LCOH$^{(wd)}$ **then** ▷ Verify lowest local LCOH
        return LCOH$^{(pv)}$
      else
        return LCOH$^{(wd)}$
      end if
    end procedure
    procedure Offshore LCOH$^{(*)}$
      if LCOH$^{(fx)}$ **then**
        use Eq. (2)$^{(fx)}$
      else if LCOH$^{(ft)}$ **then**
        use Eq. (2)$^{(ft)}$
      end if
    end procedure
  end for
end procedure ▷ Exit SGM
Deliver: LCOH$^{(*)}$

The model developed in this work assimilates learnings from past state–of–the–art articles and builds on a traditional optimisation method. The objective of the optimised general model (OGM) is to find the cheapest LCOH in a given set of suitable locations, considering hourly changing values for $\mathrm{P_{RES}}$ and $\mathrm{P_{H_2}}$. The algorithm presupposes the existence of a RES power plant and an electrolyser system in each location, with the possibility of having both solar PV and wind in a hybrid onshore configuration. The power plant's installed capacity and the electrolyser's nominal input power are the decision variables, where the latter is upper bound by the former.

The OGM is built with Pyomo [70,71], a Python–based, open–source optimisation modelling language with multiple optimisation capabilities. Pyomo sets provide indexes for parameters, variables and other sets. Coding starts with the abstract declaration of sets L and H, respectively, the eligible location points and the number of hours in one year.

Most parameters are exogenous except for the real WACC, the capital/production spread factors, and the overall cost structures. All these parameters are the same scalar for each location, apart from the capacity factors. Contrary to the yearly SGM analysis, the optimisation model needs an hourly time frame to operate correctly.

For each year's hour, the model assesses the energy production from the RES power plant and the electrolyser's rated power, evaluating which relation results in the lowest LCOH; values for onshore locations are retrieved from PVGIS tool [72] while Renewables.ninja [73,74] is used for offshore.

This model envisions the existence of three decision variables and four support variables, outlined in Table 8. While the former establishes the actual solution, the latter exists to execute auxiliary computations.

4.3.1. Mathematical formulation

Every optimisation problem requires a mathematical formalism that enables the rigorous description of the reality it is trying to model. The design of an efficient mathematical formulation rests on an understanding of how to derive innovative approaches to the architecture of the problem.

The first detail to recognise is the unique structure of the model; it consists of a very–large non–convex optimisation problem with a non–linear objective function. Such a problem may have multiple feasible regions and several locally optimal points within each region. Generally, non–convex optimisation has at least NP–hard complexity, meaning it can take time exponential in the number of variables and constraints to determine (1) that a non–convex problem is infeasible, (2) that the objective function is unbounded, or (3) that an optimal solution is the 'global optimum' across all feasible regions. Consequently,

Table 8
Summary of variables in the optimised general model.

	Variable	Index	Domain	Upper–bound	Description
Decision	P_{pv}	L	Non-Negative Reals	$P_{pv,max}$	Solar installed capacity
	P_{wd}	L		$P_{wd,max}$	Wind installed capacity
	P_{H_2}	L		$P_{pv} + P_{wd}$	Electrolyser nominal power
Support	$E_{H_2,h}$	$L,\ H$	Non-Negative Reals	$P_{pv} + P_{wd}$	Hourly electrolyser energy
	$Y_{H_2,h}$	$L,\ H$		n/a	Hourly hydrogen production
	Y_{H_2}	L			Yearly hydrogen production
	Z	L			Virtual change of variable

efforts have been made to turn the objective function from a non–linear configuration into a quadratic one, which speeds up the solving process while maintaining the validity of the results.

The following items address the definitions of the constraints and the objective function.

Constraint Expressions

The subsequent equations follow the reasoning to compute the optimised LCOH at each location; the solution then consists of the RES installed capacity values and the nominal input power of the electrolyser. Coloured elements in the expressions indicate decision variables.

- Hourly electricity consumption by the electrolyser *The hourly electricity generation is equal to the solar/wind installed capacity times the respective capacity factor; this electricity can either be directed to the electrolyser or be unused (curtailed). Thus, the electricity consumption by the electrolyser must always be less than or equal to the electricity generated by the RES.*

$$E_{H_2,h} \leq P_{pv} \times CF_{pv,h} + P_{wd} \times CF_{wd,h} \tag{10}$$

- Hourly electrolyser electricity use limit *The electrolyser input power always limits the hourly amount of electricity directed to the electrolyser.*

$$E_{H_2,h} \leq P_{H_2} \times 1\ \text{hour} \tag{11}$$

- Electrolyser nominal input power upper–bound *The electrolyser input power must be lower than the RES installed capacity.*

$$P_{H_2} \leq P_{pv} + P_{wd} \tag{12}$$

- Hourly hydrogen production *The amount of hydrogen produced in each hour is equal to the electricity directed to the electrolyser times the all–round electric efficiency and the net production rate.*

$$Y_{H_2,h} = E_{H_2,h} \times \eta \times \rho \tag{13}$$

- Lifetime discounted hydrogen production *The amount of hydrogen produced during the entire lifetime of the project is the production spread factor times the yearly sum of the hydrogen yield at each hour.*

$$Y_{H_2} = S_Y \times \sum_h Y_{H_2,h} \tag{14}$$

- Lifetime hydrogen virtual demand *The total hydrogen demand is equal to the minimum yearly hydrogen demand times the economic lifetime of the system (assumed to be 30 years). The 100 ton value considered is referenced back to the 425 kg–daily mass output of GenFuel's Plug 1 MW electrolyser [58] (adjusted for the utilisation factor).*

$$Y_{H_2} \geq 100\,000 \times 30 \tag{15}$$

- Area power density limits *The combined installed capacity of both power plants and the electrolyser must not exceed the available area. The power density of each system ($\chi_{pv} = 0.08268\,\text{kW/m}^2$, $\chi_{wd} = 0.7823\,\text{kW/m}^2$, $\chi_{H_2} = 85.32\,\text{kW/m}^2$), is computed by dividing the upper–bound installed capacity of each system by the total available area.*

$$\frac{P_{pv}}{\chi_{pv}} + \frac{P_{wd}}{\chi_{wd}} + \frac{P_{H_2}}{\chi_{H_2}} \leq \alpha \tag{16}$$

- RES installed capacity limits *The installed solar/wind capacity cannot exceed its respective limit (defined by the area available).*

$$P_{pv} \leq P_{pv,max} \qquad P_{wd} \leq P_{wd,max} \tag{17}$$

- Power lower bounds (non–negativity constraint) *Neither one of the variables can assume negative values.*

$$P_{pv} \geq 0 \qquad P_{wd} \geq 0 \qquad P_{H_2} \geq 0 \tag{18}$$

- Change of variable in the objective function *For the reasons expressed in Section 4.3.1, the original non–linear objective function is converted into a quadratic formula.*

$$Z \times Y_{H_2} = K_{RES} + K_{H_2} \tag{19}$$

Objective Function

The optimisation model concludes with the formulation of the objective function. Primarily, the objective is to minimise the levelised cost of hydrogen. Since this is a deterministic optimisation—in which every point is independent of the adjacent ones—, it is possible to perform a joint minimisation of all eligible locations, where the minimisation of the sum is equal to the sum of the minimisations. Eq. (20) displays the function for just one point, as it is used in the case under study.

$$\mathbf{min}\,\mathrm{LCOH} = \mathbf{min}\,\frac{K_{RES} + K_{H_2}}{Y_{H_2}} = \mathbf{min}\,Z \tag{20}$$

s.t. Equations (10) – (19)

Algorithm 2 outlines a tabulated form of the optimisation detailed process in pseudo-code.

5. Results

Following the methodologies examined in the previous chapters, the set of results is presented and examined below.

5.1. Electricity generation potential

Locations with a lower levelised cost of electricity are generally correlated with higher suitability for green hydrogen projects—thus the relevance of identifying such regions. The LCOE is computed using Eq. (9), with the expenses' values summarised in Table 9.

Fig. 5 displays the present levelised cost of electricity in the suitable locations of both countries. Most of the territory is filled with solar PV since its CapEx and OpEx are close to half and one–third that of wind, respectively. Moreover, both countries have exceptional solar irradiance during the year, which leads to higher capacity factors and

Table 9
Summary of project expenses for every renewable energy source.

	CapEx (EUR_{2020}/kW)				OpEx (EUR_{2020}/kW/yr)		
	Hardware	Balance of system	Soft costs	TOTAL	General operations	Maintenance and services	TOTAL
Solar Photovoltaic	190.26	260.19	179.55	**630**	7.63	3.27	**10.89**
Onshore Wind	819.21	255.64	87.15	**1162**	18.52	18.52	**37.04**
Offshore Fixed	797.47	659.45	247.08	**1704**	57.97	3.05	**61.02**
Offshore Floating	800.31	2303.60	501.10	**3605**	62.18	3.27	**65.45**

Algorithm 2 Optimised General Model algorithm

Require: $P_{pv,max}$, χ_{pv}, CF_{pv}, $P_{wd,max}$, χ_{wd}, CF_{wd}, χ_{H_2}, α, $\mathcal{D}$, N, S_Y ▷ Parameters of the model
1: **procedure** OGM(↩)
2: **for all** $h \in \mathbb{H}$ **do**
3: P_{pv}, P_{wd}, P_{H_2} ← ▷ Set initial guesses for decision variables
4: **Ensure:** $0 \leq P_{pv} \leq P_{pv,max}$
5: $0 \leq P_{wd} \leq P_{wd,max}$
6: $0 \leq P_{H_2} \leq P_{pv} + P_{wd}$
7: $P_{pv} : \chi_{pv} + P_{wd} : \chi_{wd} + P_{H_2} : \chi_{H_2} \leq \alpha$
8: $P_{pv} \times CF_{pv,h} + P_{wd} \times CF_{wd,h} = E_{H_2,h}$ ▷ Compute electricity use by the electrolyser
9: **if** $E_{H_2,h} \geq P_{H_2}$ **then**
10: **return** *to line 3:*
11: *decrease* P_{pv} *or* P_{wd}
12: **else**
13: $E_{H_2,h} \times \rho \times \eta = Y_{H_2,h}$ ▷ Compute hydrogen production
14: **end if**
15: $Y_{H_2} = S_Y \times \sum_h Y_{H_2,h}$
16: **end for**
17: $\mathcal{D}$ ← ▷ Set hydrogen virtual demand
18: **Ensure:** $Y_{H_2} \geq \mathcal{D} \times N$
19: **procedure** LCOH(⊙)
20: *use* Eq. (2)
21: **end procedure**
22: **end procedure** ▷ Exit OGM
Deliver: $P^{\odot}_{pv}$, $P^{\odot}_{wd}$, $P^{\odot}_{H_2}$, $LCOH^{\odot}$

further favours solar LCOE. The dominance of cheap onshore production is evident, with LCOEs oscillating between 17.43 EUR_{2020}/MWh to 37.45 EUR_{2020}/MWh in Portugal and 22.28 to 40.43 EUR_{2020}/MWh in Italy.

On the contrary, offshore wind with floating devices is still the most expensive of these technologies to produce electricity nowadays, with LCOEs as high as 110 EUR_{2020}/MWh in Portugal and 435 EUR_{2020}/MWh in Italy. This fact is due to the technology's very high capital and operational expenditures, as well as the low capacity factors of some regions.

5.2. Hydrogen production potential

The oversize factor must first be determined to meaningfully assess the potential for extensive hydrogen production. This ratio between the RES installed capacity and the electrolyser is computed to yield the lowest LCOH in each suitable location. With no access to enough computational power to optimise the whole country, the algorithm is instead run in three points per technology for each country—with the chosen locations reflecting every set's minimum, average and maximum capacity factors. Table 10 outlines the results of said simulations.

LCOH is the levelised cost of hydrogen computed by the oversimplified model (with $P_{RES} = P_{H_2}$), while **LCOH⊙** is the outcome of the optimisation model. **GAP** shows the percentage improvement of the previous results. $\mathbf{P_{RES}}$ and $\mathbf{P_{H_2}}$ are, respectively, the resulting RES installed capacity and the electrolyser's nominal input power. Finally, the **Oversize Factor** is obtained after dividing these last two entities.

The next step is to plot this factor against the technologies considered to find a relation that can be used in the remaining points. Fig. 6 shows just that, identifying the average oversize factor as the centroid of the results of the same technology. Note how this value decreases almost linearly with the renewable energy sources presented.

Apparently, there is an inverse correlation between the oversize factor and one such entity that increases going from onshore to close–off shore, to far–offshore: most likely, the capacity factor. Fig. 7 now shows the oversize factor plotted against the full load hours of each of the previous locations' systems. Thereby, the correlation is evident, although not entirely accurate—the green trendline is a power curve with $R^2 = 0.6467$.

A close examination of these charts determines the independence of the results from the chosen countries, i.e. Italy and Portugal have optimisation results that support this correlation. Given the potential similarities between the two territories, whether this conclusion stems from any coincidence remains to be confirmed. More research on this subject should be done using the same methodology in more locations across these and other nations' borders to achieve a clearer and more accurate relationship. However, this method provides an initial precise approximation of a more realistic model—that is, a more accurate model than the oversimplified solution. Consequently, the remaining points related to each technology's LCOH are calculated using the centroid values shown in Fig. 6.

Fig. 8 maps out the current overall levelised cost of hydrogen in both Portugal and Italy.

A direct comparison can be made between the two countries, with the initial caveat that the colour–spectrum scale of the legend is not the same.

Either way, the LCOH is generally lower onshore than offshore; in Portugal, onshore costs average at 6.85 EUR/kg, while in Italy, the average is 7.25 EUR/kg (as opposed to 10.48 EUR/kg and 15.81 EUR/kg, respectively, offshore). While the main reason for the disparity between on/offshore costs is the cost structure of each technology, the primary cause for the discrepancy in values between the two countries is related to solar and wind exposure.

Both countries have a distinct North–South divide in terms of solar exposure. The South receives more sunlight overall; this is particularly true of Sicily in Italy and the Algarve and Alentejo regions of Portugal, where FLH values regularly approach 1700 h. Not so much in the Centre and North zones, which only reached slightly over 1000 full load hours. However, Portugal has a few northern areas that receive a lot of sunlight, particularly those near the coast and the eastern border. This feature is the main justification previously offered for the lower LCOH average.

Concerning wind exposure, there is a crucial acknowledgement of the differences between onshore and offshore locations. Particularly in Portugal, there are notable differences between the average onshore load factor of 2423 h and the average locations in its exclusive economic zone of 4200 FLH. Italy does not experience this phenomenon

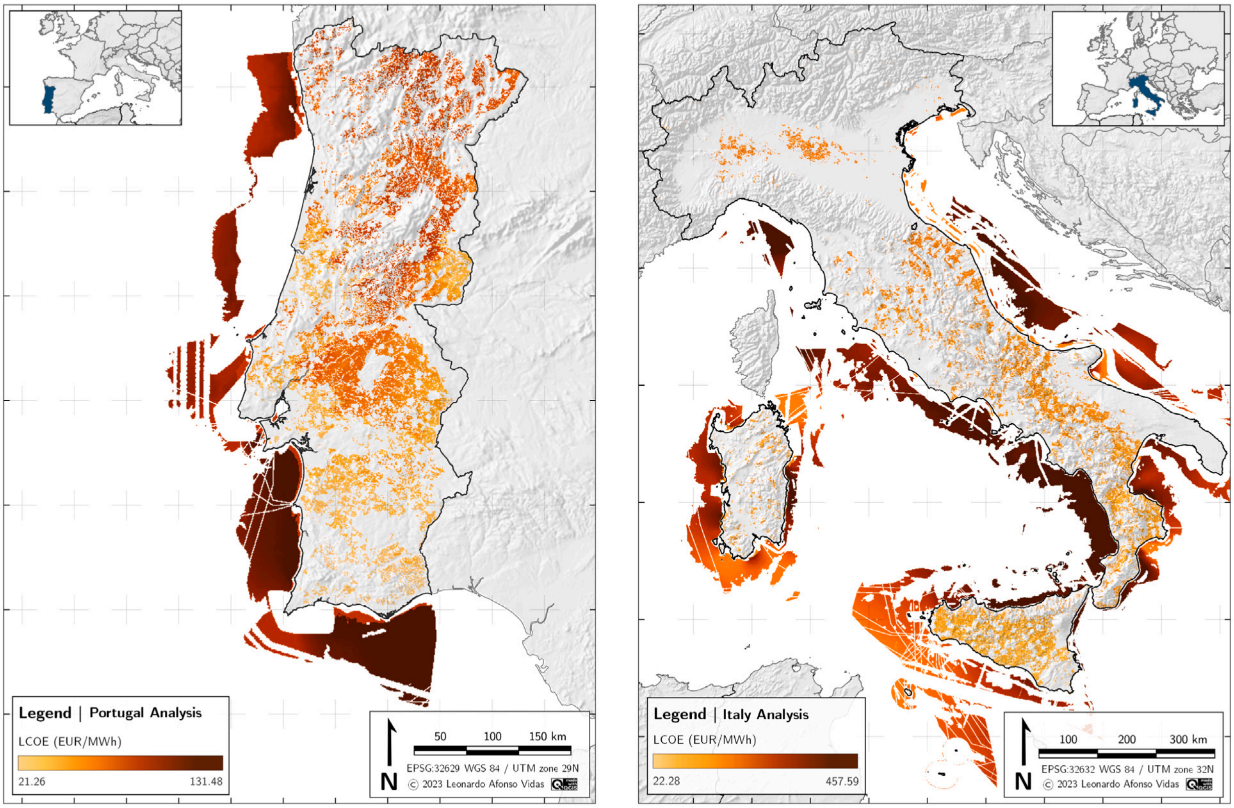

(a) Portugal (b) Italy

Fig. 5. Current levelised cost of electricity in eligible locations of selected countries.

Table 10
Summary of results: optimisation algorithm.

		Technology		— Point Location — LAT	LON	LCOH (EUR/kg)	$LCOH^{\odot}$ (EUR/kg)	GAP (%)	$P^{\odot}_{RES}$ (MW)	$P^{\odot}_{H_2}$ (MW)	Oversize Factor
ITALY	Onshore	Solar	I	36°45′21.87″	11°59′32.45″	10.89	8.05	26.08	50.27	25.81	1.95
		Solar	II	41°11′35.24″	15°21′54.14″	12.41	9.08	28.83	37.30	18.17	2.05
		Solar	III	46°10′7.52″	12°0′20.73″	13.28	9.64	27.41	27.89	13.35	2.09
		Wind	I	36°45′21.87″	11°59′32.45″	4.57	4.54	0.66	2.51	2.51	1.00
		Wind	II	41°11′35.24″	15°21′54.14″	13.18	12.29	6.75	206.44	129.37	1.59
		Wind	III	46°10′7.52″	12°0′20.73″	19.13	18.81	1.67	309.17	143.37	2.16
	Offshore	Fixed	I	41°11′58.16″	9°33′11.76″	16.41	16.12	1.77	12.07	10.02	1.20
		Fixed	II	42°0′14.88″	15°32′56.79″	22.48	21.05	6.36	56.09	35.34	1.58
		Fixed	III	45°41′49.34″	13°32′0.06″	25.19	24.36	3.30	7.73	6.03	1.28
		Float	I	41°34′3.17″	11°7′40.84″	23.56	23.53	0.12	85.97	84.25	1.02
		Float	II	41°18′44.71″	8°33′59.20″	31.02	30.90	0.39	29.49	27.43	1.08
		Float	III	43°19′39.62″	9°37′13.07″	37.93	37.72	0.55	11.66	10.49	1.11
PORTUGAL	Onshore	Solar	I	37°6′56.93″	−8°26′2.17″	10.26	7.79	24.07	25.43	13.09	1.94
		Solar	II	40°12′20.77″	−8°0′20.88″	12.27	9.02	26.49	50.28	25.10	2.00
		Solar	III	41°52′29.78″	−7°41′54.12″	12.31	9.03	26.65	16.89	7.99	2.11
		Wind	I	37°6′56.93″	−8°26′2.17″	5.02	4.98	0.79	93.17	87.23	1.07
		Wind	II	40°12′20.77″	−8°0′20.88″	23.12	19.96	13.67	72.43	33.74	2.15
		Wind	III	41°52′29.78″	−7°41′54.12″	28.18	23.97	14.93	65.57	31.56	2.07
	Offshore	Fixed	I	39°14′47.66″	−9°23′3.84″	15.06	14.44	4.12	103.61	73.56	1.41
		Fixed	II	41°28′3.53″	−8°48′31.51″	21.68	20.32	6.27	139.88	89.84	1.56
		Fixed	III	36°58′39.17″	−7°48′14.35″	24.62	21.93	10.93	391.63	211.13	1.85
		Float	I	38°33′22.72″	−9°41′38.46″	16.53	16.46	0.42	51.43	47.83	1.08
		Float	II	37°46′40.66″	−9°8′46.95″	15.35	15.27	0.52	11.92	10.93	1.09
		Float	III	36°58′13.86″	−7°48′14.75″	36.05	34.24	5.02	11.39	7.52	1.51

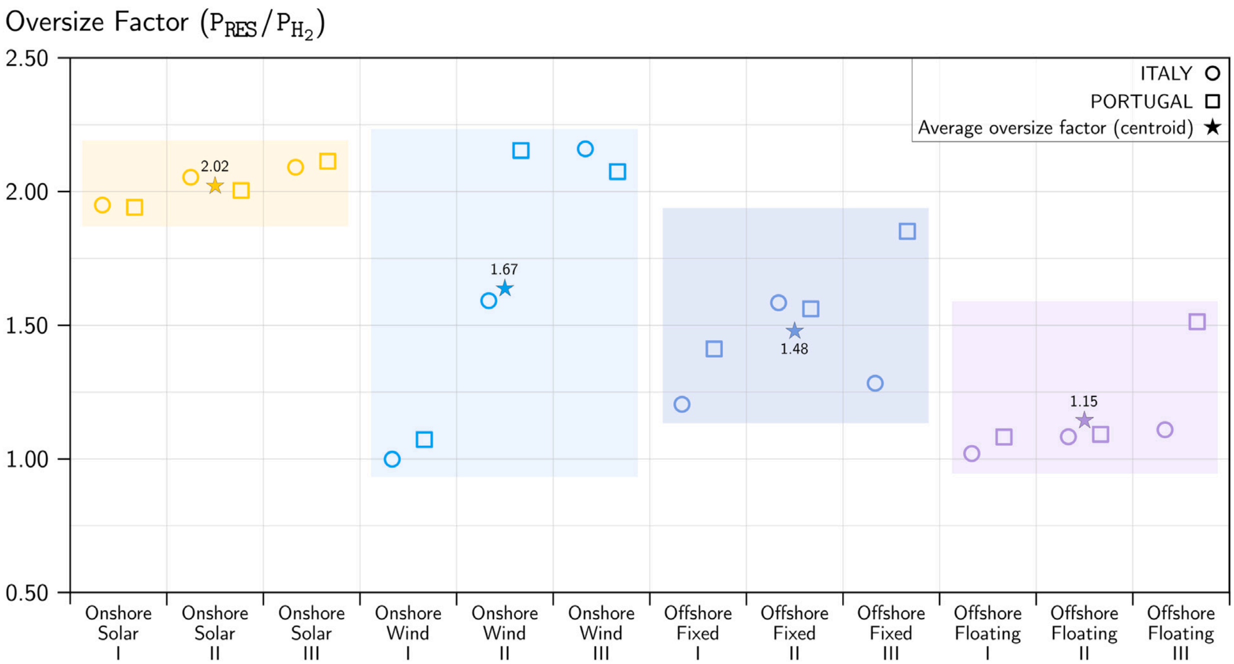

Fig. 6. Oversize factor as function of RES technology.

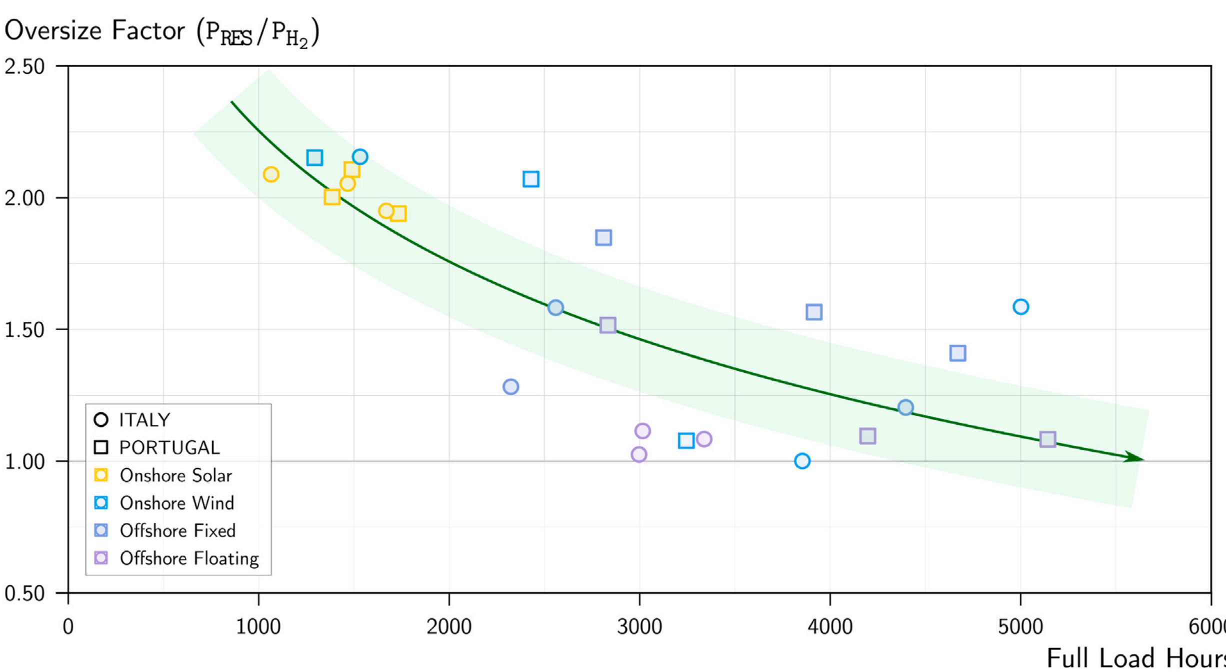

Fig. 7. Oversize factor as function of RES full load hours.

to the same extent, possibly because its EEZ is confined within the Mediterranean Sea rather than in the open Atlantic Ocean. Reduced roughness lengths associated with protruding landscapes affecting wind patterns are necessary for higher wind speeds. Therefore, the onshore/offshore average is not all that different, with 2103 FLH for the former and 2995 FLH for the latter, despite the fact that the entire coast of Sardinia and the west coast of Sicily exhibit higher capacity factors.

In addition to the results obtained from the traditional optimisation process, the model is further used to perform a specialised hybrid optimisation in selected onshore locations of both countries.

Table 11 summarises the outcomes of such optimisation.

This procedure aims to join both onshore technologies in the same location and compute each installed capacity to minimise the levelised cost of hydrogen.

In Table 11, the simplified solar/wind LCOH is first provided for every point and then the optimised LCOH, followed by each technology's nominal power. As expected, **LCOH**$^{\circledcirc}$ is always (much) lower than any individual **LCOH**, which inherently validates the model.

Another relevant aspect to notice in these results is the predominant correlation of the preferred RES technology and the respective **LCOH**;

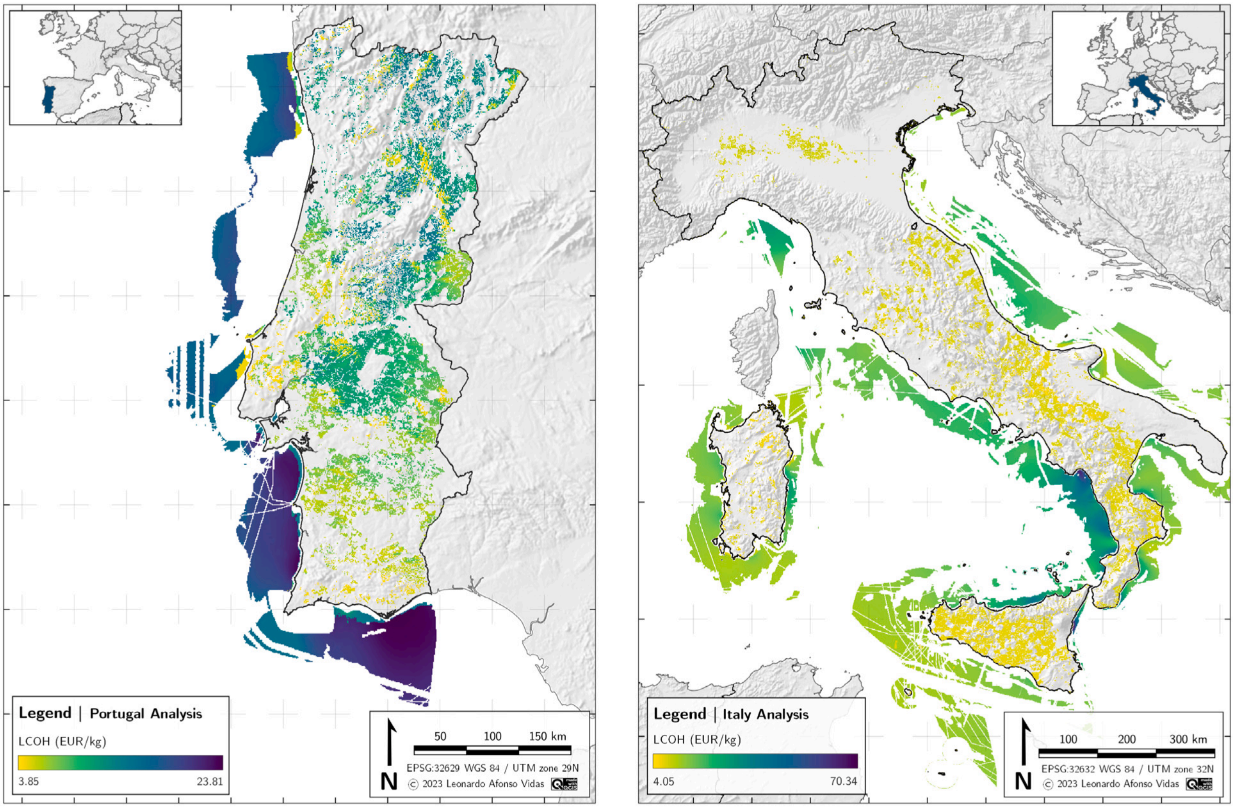

(a) Portugal (b) Italy

Fig. 8. Current levelised cost of hydrogen in eligible locations of selected countries.

Table 11
Summary of results: hybrid optimisation.

	Onshore technology		— Point Location —		LCOH (EUR/kg)	$LCOH^{\odot}$ (EUR/kg)	$P^{\odot}_{pv}$ (MW)	$P^{\odot}_{wd}$ (MW)	$P^{\odot}_{H_2}$ (MW)
			LAT	LON					
ITALY	Solar Wind	I	36° 45′21.87″	11° 59′32.445″	10.89 4.57	**3.73**	0.01	164.90	164.59
	Solar Wind	II	41° 11′35.243″	15° 21′54.14″	12.41 13.18	**7.74**	10.59	7.06	7.07
	Solar Wind	III	46° 10′7.516″	12° 0′20.729″	13.28 19.13	**9.15**	41.84	0.03	20.87
PORTUGAL	Solar Wind	I	37° 6′56.929″	−8° 26′2.165″	10.26 5.02	**4.06**	1.77	7.24	7.06
	Solar Wind	II	40° 12′20.773″	−8° 0′20.882″	12.27 23.12	**8.57**	27.48	0.00	14.01
	Solar Wind	III	41° 52′29.78″	−7° 41′54.121″	12.31 28.18	**8.58**	20.95	0.10	10.41

i.e., for each location, the renewable source with the lowest **LCOH** is the one that later has the highest installed capacity in the $\mathbf{LCOH}^{\odot}$ computation. Moreover, $\mathbf{P}_{\mathbf{H_2}}$ is always smaller than the sum of $\mathbf{P}_{\mathbf{pv}}$ and $\mathbf{P}_{\mathbf{wd}}$, as initially constrained.

To better understand the scale of improvement provided by the optimisation algorithm, Fig. 9 illustrates the central columns of Table 11 as a bar chart.

The yellow and blue bars respectively depict the LCOH from solar and wind systems alone, while the green bars represent the optimised hybridisation of both technologies. The true power of the algorithm is evident in the relative reductions displayed; in the specific case of these locations, it can be as high as 70%—it could be even higher for other locations not addressed in this analysis. These reductions may lead to savings to the project owner in the order of €2 million for just a 100–ton annual demand.

6. Discussion

With results presented and examined, it remains only to discuss potential improvements to the analysis and perform sensitivity analysis for the most relevant parameters of the economic model to put them into perspective.

6.1. Potential improvements

While this analysis has been conducted to the best of the authors' knowledge and capabilities, a few points were identified as plausible betterment to the overall work:

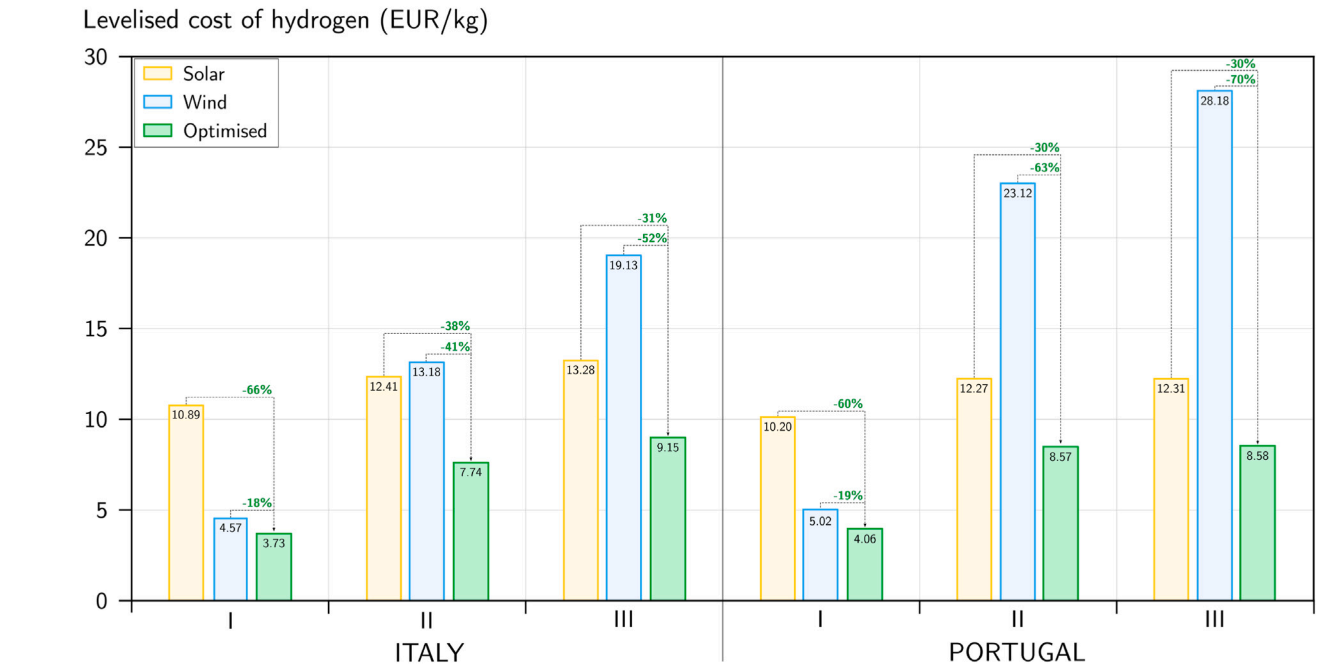

Fig. 9. Onshore hybrid optimisation.

- Other renewables could have been considered for the computation of the LCOE and, consequently, the LCOH. Hydropower, geothermal energy, and even nuclear energy could be good allies to hydrogen production, especially because of their baseload profile, which would greatly improve hydrogen annual production and decrease its unitary cost.
- On the geographical model design, a different weight could have been attributed to each exclusion and evaluation criterion according to local preferences. This method would yield more accurate eligible locations on a regional level, but it would be harder to implement countrywide.
- On the numerical model layout, the storage and transportation costs could have been considered when studying the hydrogen economic fairways. These additions would bring a more comprehensive view of the real project, although being very dependent on regional supply and local demand.
- When computing the optimised levelised cost of hydrogen, namely for hybrid configurations, enough computational power would be useful to perform the analysis for the whole countries.

6.2. Sensitivity analysis

Any benchmark economic analysis benefits from an in–depth sensitivity analysis.

In the particular case of this work, the objective variable is the levelised cost of hydrogen; its sensitivity is tested against several input parameters, comprised of the most significant variables of the economic model.

Each parameter is alternately subjected to a relative variation of −50% to + 50%, in intervals of 10%. The LCOH variance is computed through a traditional relative percentage error formula for each evaluation.

The process is repeated for the four RES technologies, whose results are illustrated in the following charts; Fig. 10 shows the results of the sensitivity analysis applied to solar LCOH, while Figs. 11–13 respectively refer to onshore wind and offshore wind with fixed foundations and floating devices.

At first glance, three distinct groups can be discerned: one comprising the full load hours, the economic life of the project and inflation, which are inversely proportional to the levelised cost of hydrogen; a second group that consists of both degradations, both operational expenses and the electrolyser replacement cost, which directly affect the LCOH but no more than 10%; and a third group, including both capital expenditures and the nominal WACC, that directly impact the LCOH by more than 10%.

Concerning these charts, FLH is evidently the predominant variable that most influences the LCOH. The project lifetime and inflation are the subsequent most relevant variables, respectively varying the levelised cost of hydrogen by up to 40% and 10% when reduced to half. It makes sense that the LCOH would vary inversely with these three parameters since (1) a lower capacity factor leads to less energy being generated and less hydrogen being produced for the same plant capacity—thus increasing the share of the overall cost structures; (2) a shorter economic life gives projects limited time for the production to compensate the investment costs, then increasing each unit–cost of hydrogen; and (3) a lower inflation rate means diminished differences between total expenditures and global hydrogen yield, which removes the advantage of locking energy ‘costs’ at a constant initial rate.

In the next group of variables, degradation rates and operational expenses represent the most negligible influences of all; future reductions of up to 50% in these variables would only decrease the LCOH by about 5%. Therefore, although necessary, this should not be the focus of forthcoming developments.

Finally, the third group, comprising capital expenditures and nominal WACC, makes up the set of input parameters that directly impact hydrogen’s levelised cost the most. Expected reductions in turbine/module and electrolyser CapEx can lead to hydrogen being 20% cheaper.

For offshore technologies, the general look is similar to the previous ones; the fundamental disparities concern the last two aforementioned groups. Here, they are not as well defined as before but instead seem to merge into a single extended group with relative variations ranging from less than 1% to more than 30%. Both turbine and electrolyser degradations and operational expenses continue to be the least impactful parameters.

On the other hand, the variables with the most significant influence are the electrolyser CapEx, the nominal WACC and the RES CapEx. The latter is especially relevant to offshore floating devices, with the highest

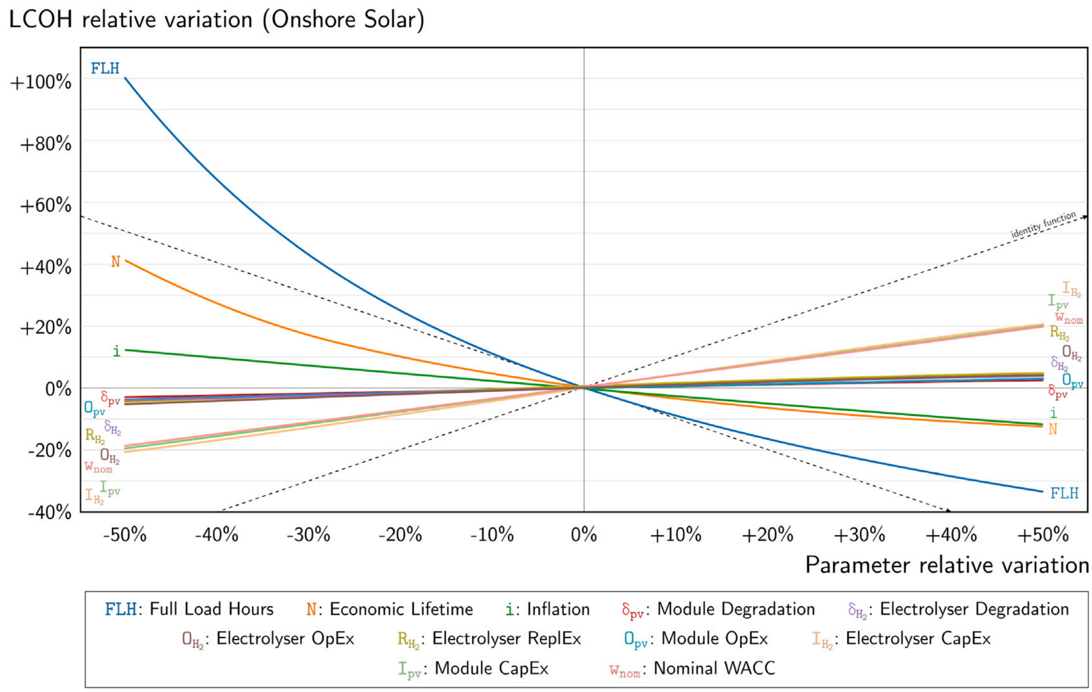

Fig. 10. Sensitivity analysis: onshore solar.

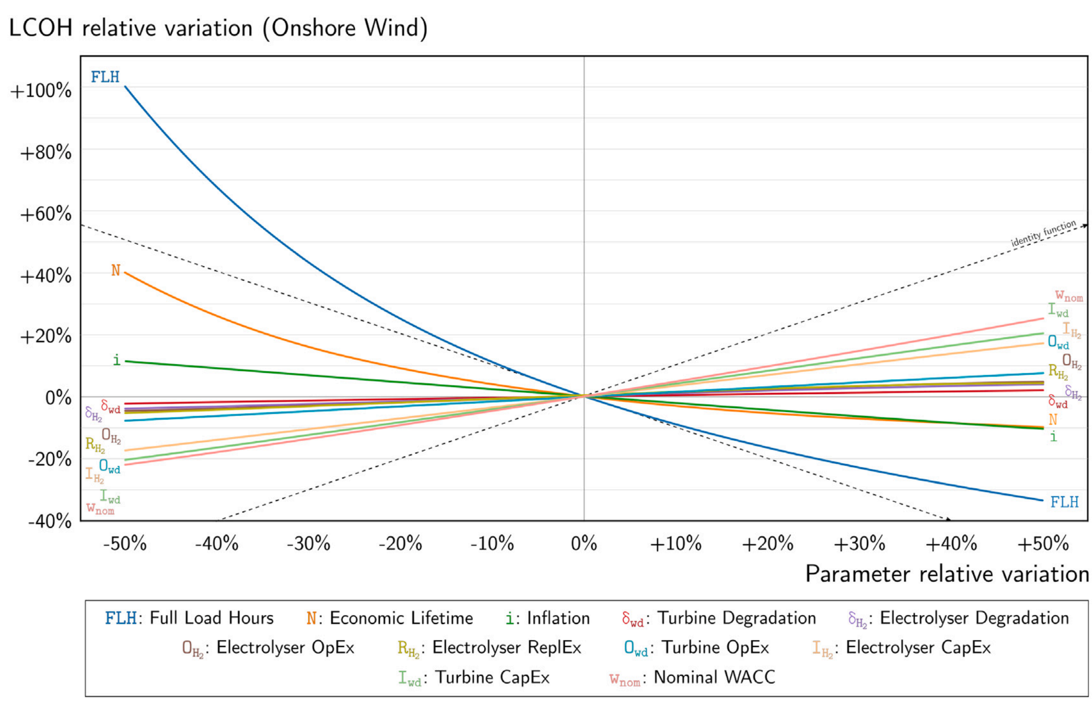

Fig. 11. Sensitivity analysis: onshore wind.

capital expenditures of all RES considered. Hence, future research aimed at decreasing this LCOH component should be incentivised.

Two more important elements remain to be analysed: the electrolyser electric efficiency (η) and net production rate (ρ). Fig. 14 illustrates both variables as a set of four superimposed curves, one for each RES technology. These two parameters undoubtedly show the most considerable potential for improvement on the LCOH; when combined, even small positive developments can lead to steep decreases in the future cost of producing hydrogen—thus, should be placed at the forefront of electrolyser development research.

7. Conclusions

This study intended to find the configurations of renewable energy sources and electrolysers that return the lowest lifetime production cost in specific available locations while also obtaining a preliminary oversize factor to apply in extensive geographical analyses. It starts by examining the economic fairways of hydrogen in such locations and computing the levelised cost of hydrogen through an extensive sequence of formulations. A simplified general model is created per present–day international literature, based on the maximum allowed capacity of the

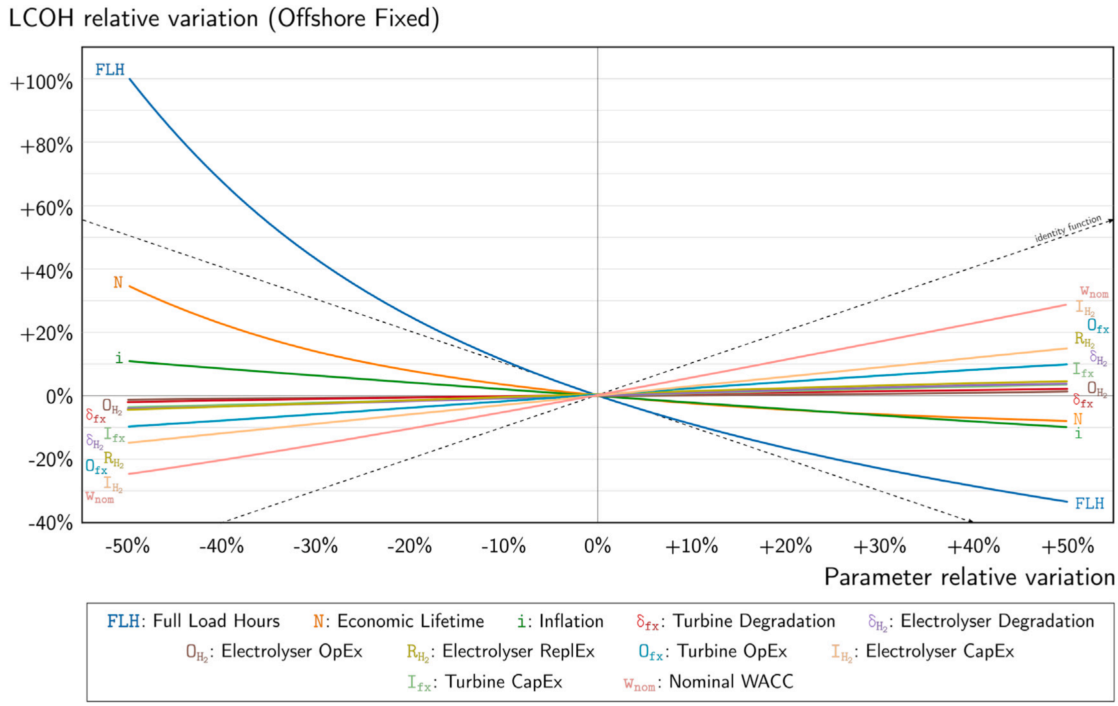

Fig. 12. Sensitivity analysis: offshore fixed.

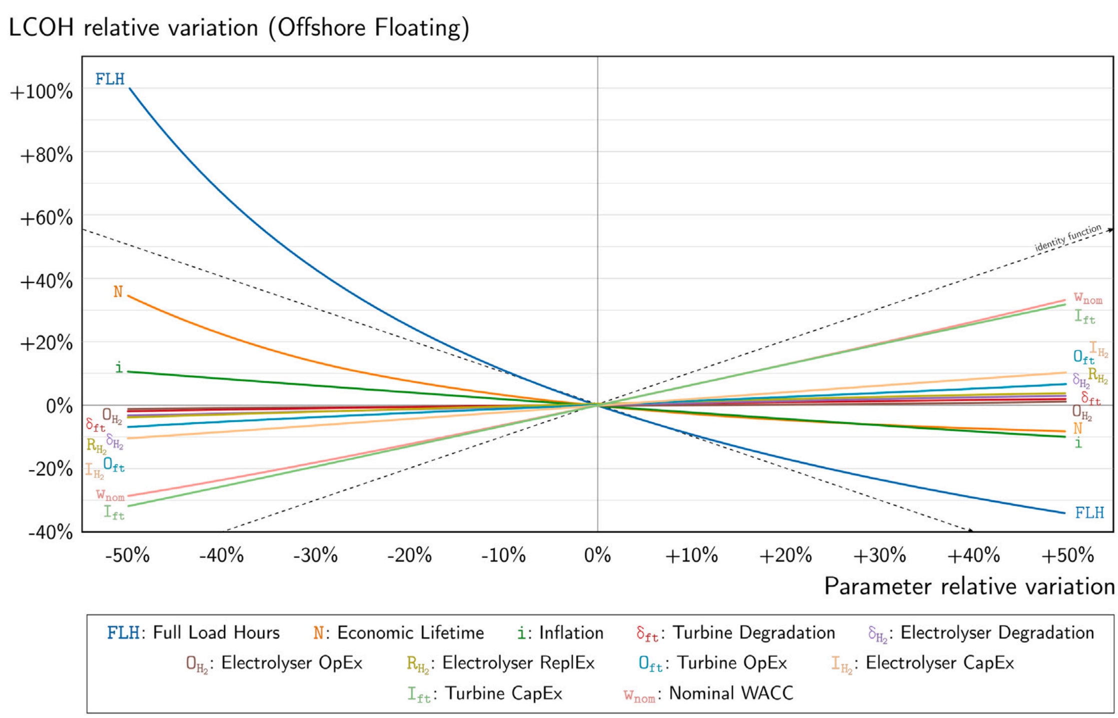

Fig. 13. Sensitivity analysis: offshore floating.

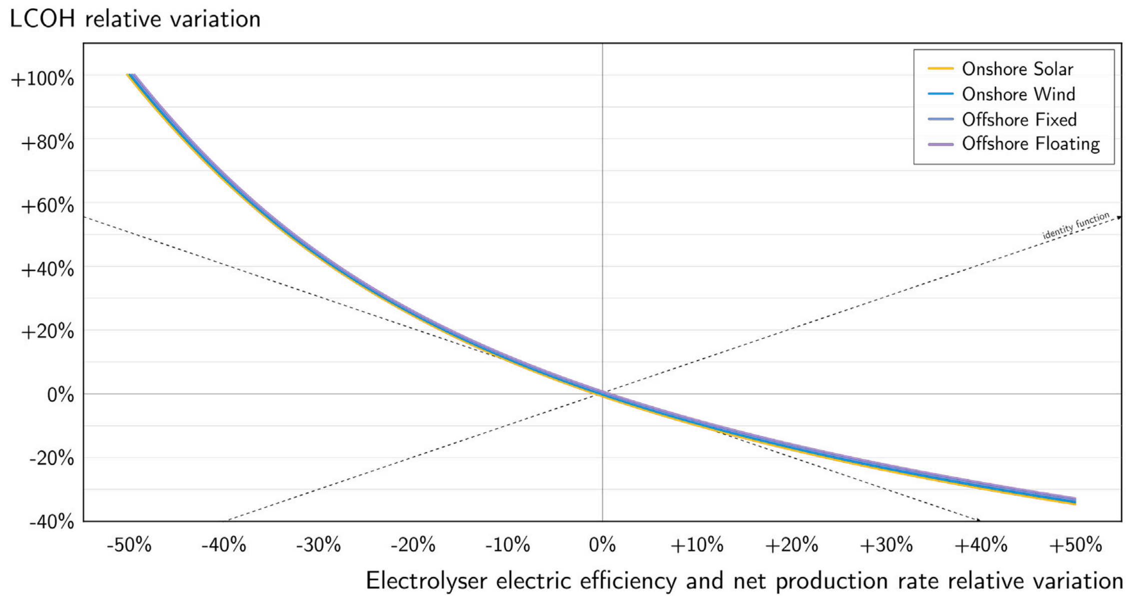

Fig. 14. Sensitivity analysis: electrolyser efficiency and production rate.

renewable power plants. Still, this model improves on the existing ones by using an oversize factor determined via an optimisation algorithm. Regarding this finding, the main conclusions are:

- There is an apparent inverse correlation between the oversize factor and the full load hours of the renewable energy system contemplated. This means that for RES technologies with higher capacity factors, the coupled electrolyser should approximate the size of the renewable power plant.
- Using this factor, the LCOH generally yields lower values onshore than offshore. The averages for Italy and Portugal are respectively 7.25 EUR/kg and 6.85 EUR/kg (onshore), 15.81 EUR/kg and 10.48 EUR/kg (offshore).
- The fundamental cause of disparity between onshore and offshore values is the cost structure of each technology; the leading explanation for the value discrepancy between both countries is solar/wind exposure. The capacity factor is one of the most predominant aspects affecting the levelised cost of hydrogen.

Introducing this oversize factor significantly improved the study's credibility, producing results ever closer to reality. This procedure constructively challenges the standard way of assessing large–scale green–hydrogen projects and thus may be replicated in subsequent analyses as a means to make estimations better resemble the real world.

Lastly, the algorithm developed to obtain the oversize factor, as part of the optimised general model, is one of this analysis' major outcomes. Its foundation is grounded on a comprehensive problem setting and mathematical formulation, comprising the detailed definition of index sets, parameters, support and decision variables, and an objective function constrained by several equations. When used on a country–specific set of points, the following was concluded:

- Single configurations obtained LCOH reductions in Italy and Portugal of up to 7% and 11% (offshore) and 29% and 27% (onshore), respectively. Such cutbacks could translate to millions of euros in savings for the project investors, depending on the established hydrogen demand.
- Hybrid onshore configurations, where both solar and wind power plants are connected to the electrolyser, generated the highest reductions in the cost of producing hydrogen—the LCOH decreased as much as 52% in Italy and 70% in Portugal. Reductions such as these could significantly impact the economics of any project.

These results validate the initial premise of the algorithm in providing the optimal computation of the levelised cost of hydrogen with notable success. A model with such attributes has yet to be found in the literature, evidencing its important contribution to addressing this gap.

In the end, an in–depth sensitivity analysis of the economic model is presented, encompassing five symmetric relative variations of 11 parameters assigned to each RES. The tests originated three unique groups of variables:

- The first group, including the FLH, the electrolyser electric efficiency and net production rate, the project's economic lifetime and inflation, inversely affect the LCOH the most—ranging from + 100% to −32%.
- The second group comprises the nominal WACC and both systems' CapEx, and most directly impact the LCOH—from −32% to + 39%.
- The third group, containing both system' degradation rates and OpEx, and the replacement cost of the electrolyser, has the least impact on the levelised cost of hydrogen—from −7% to + 8%.

As a concluding remark, one has to acknowledge that the evidence base is fast–moving, and so there can be expected gaps in the knowledge. Nonetheless, this work improves on the body of research published so far and contributes to developing this field of study.

CRediT authorship contribution statement

Leonardo Vidas: Conceptualization, Data curation, Investigation, Methodology, Software, Original draft. **Rui Castro:** Conceptualization, Formal analysis, Funding acquisition, Methodology, Project administration, Resources, Supervision, Validation, Visualization, Review & editing. **Alessandro Bosisio:** Conceptualization, Formal analysis, Funding acquisition, Methodology, Project administration, Resources, Supervision, Validation, Visualization, Review & editing. **Armando Pires:** Formal analysis, Validation, Visualization, Review & editing.

Declaration of competing interest

The authors declare that they have no known competing financial interests or personal relationships that could have appeared to influence the work reported in this paper.

Data availability

Data will be made available on request.

Acknowledgements

Rui Castro was supported by National funds through FCT, Fundação para a Ciência e a Tecnologia, Portugal, under project UIDB/50021/2020

A. J. Pires was supported by National funds through FCT, Fundação para a Ciência e a Tecnologia, Portugal, under project UIDB/00066/2020

References

[1] International Renewable Energy Agency. Geopolitics of the energy transformation: the hydrogen factor. Technical report ISBN: 978-92-9260-370-0, Abu Dhabi: International Renewable Energy Agency; 2022.
[2] Vidas L, Castro R, Pires A. A review of the impact of hydrogen integration in natural gas distribution networks and electric smart grids. Energies 2022. http://dx.doi.org/10.3390/en15093160.
[3] International Energy Agency. The future of hydrogen. Technology report, International Energy Agency; 2019, Available online: https://www.iea.org/reports/the-future-of-hydrogen. [Accessed on 21 July 2022].
[4] International Renewable Energy Agency. Hydrogen: A renewable energy perspective. Technology report ISBN: 978-92-9260-151-5, Abu Dhabi: International Renewable Energy Agency; 2019.
[5] Franco BA. Techno-economic assessment of hydrogen offloading systems for offshore wind farms. [Master's thesis], Instituto Superior Técnico; 2020, Available online: https://fenix.tecnico.ulisboa.pt/cursos/mege/dissertacao/846778572212432. [Accessed on 26 August 2022].
[6] Narayan KR. Hydrogen-powered long-distance transportation for portugal. [Master's thesis], Instituto Superior Técnico; 2021, Available online: https://fenix.tecnico.ulisboa.pt/cursos/mege/dissertacao/846778572212854. [Accessed on 26 August 2022].
[7] Groenewegen C. GIS-based site suitability analysis for solar and win to hydrogen potential in Europe and Mediterranean region in 2030 and 2040. Delft University of Technology; 2021, Available online: https://repository.tudelft.nl/islandora/object/uuid:08a61dd0-21c0-496b-8db9-f43642f9054c. [Accessed on 08 August 2022].
[8] Vagiona DG, Kamilakis M. Sustainable site selection for offshore wind farms in the south Aegean—Greece. Sustainability 2018. http://dx.doi.org/10.3390/su10030749.
[9] Juárez-Casildo V, Cervantes I, de G. González-Huerta R. Solar hydrogen production in urban areas of Mexico: towards hydrogen cities. Int J Hydrog Energy 2022. http://dx.doi.org/10.1016/j.ijhydene.2022.06.137.
[10] Raillani B, Mezrhab A, Amraqui S, Moussaoui MA, Mezrhab A. Regression-based spatial GIS analysis for an accurate assessment of renewable energy potential. Energy Sustain Development 2022. http://dx.doi.org/10.1016/j.esd.2022.06.003.
[11] Pandora Gkeka-Serpetsidaki and Theocharis Tsoutsos. A methodological framework for optimal siting of offshore wind farms: A case study on the island of Crete. Energy 2022. http://dx.doi.org/10.1016/j.energy.2021.122296.
[12] Gunawan TA, Singlitico A, Blount P, Burchill J, Carton JG, Monaghan RFD. At what cost can renewable hydrogen offset fossil fuel use in Ireland's gas network? Energies 2020. http://dx.doi.org/10.3390/en13071798.
[13] Atlam O, Barbir F, Bezmalinovic D. A method for optimal sizing of an electrolyzer directly connected to a PV module. Int J Hydrog Energy 2011. http://dx.doi.org/10.1016/j.ijhydene.2011.03.073.
[14] Eichman J, Koleva M, Guerra OJ, McLaughlin B. Optimizing an integrated renewable electrolysis system. Technical report NREL/TP-5400-75635, TN 37831-0062, USA: National Renewable Energy Laboratory; 2020.
[15] Jiang Y, Huang W, Yang G. Electrolysis plant size optimization and benefit analysis of a far offshore wind-hydrogen system based on information gap decision theory and chance constraints programming. Int J Hydrog Energy 2022. http://dx.doi.org/10.1016/j.ijhydene.2021.11.211.
[16] Scolaro M, Kittner N. Optimizing hybrid offshore wind farms for cost-competitive hydrogen production in Germany. Int J Hydrog Energy 2022. http://dx.doi.org/10.1016/j.ijhydene.2021.12.062.
[17] Gunawan TA, Singlitico A, Blount P, Carton JG, Monaghan RF. Towards techno-economic evaluation of renewable hydrogen production from wind curtailment and injection into the irish gas network. In: Proceedings of ECOS 2019, The 32nd international conference on efficiency, cost, optimization, simulation and environmental impact of energy systems. Wroclaw, Poland, 2019.
[18] Ali F, Bennui A, Chowdhury S, Techato K. Suitable site selection for solar-based green hydrogen in southern thailand using GIS-MCDM approach. Sustainability 2022. http://dx.doi.org/10.3390/su14116597.
[19] QGIS Development Team. QGIS geographic information system. QGIS Association; 2022, URL https://www.qgis.org.
[20] MapTiler Team. EPSG:32632 - WGS 84/UTM zone 32N. 2022, Available online: https://epsg.io/32632. [Accessed on 04 June 2022].
[21] MapTiler Team. EPSG:32629 - WGS 84/UTM zone 29N. 2022, Available online: https://epsg.io/32629. [Accessed on 04 June 2022].
[22] Carlos Efraín Porto Tapiquén. Geografía, SIG y Cartografí a Digital. 2022, Available online: http://www.efrainmaps.es. [Accessed on 05 June 2022].
[23] Hijmans RJ. Boundary of Italy. 2015, Available online: https://earthworks.stanford.edu. [Accessed on 31 March 2022].
[24] European Environment Agency. Hillshade Europe DEM. 2004, Available online: https://www.eea.europa.eu/data-and-maps. [Accessed on 13 April 2022].
[25] Hijmans RJ. First-level administrative divisions of Italy. 2015, Available online: https://earthworks.stanford.edu. [Accessed on 01 April 2022].
[26] ICPAC Geoportal. Africa - admin level 0. 2017, Available online: http://geoportal.icpac.net. [Accessed on 05 June 2022].
[27] European Marine Observation and Data Network. Exclusive economic zone areas in European seas. 2021, Available online: https://www.emodnet-humanactivities.eu/. [Accessed on 3 May 2022].
[28] ForestGIS. 2022, Available online: https://forest-gis.com/shapefiles-de-portugal/. [Accessed on 16 May 2022].
[29] EMODnet Bathymetry Consortium. Emodnet digital bathymetry (DTM 2020). 2020, http://dx.doi.org/10.12770/bb6a87dd-e579-4036-abe1-e649cea9881a.
[30] European Commission, Directorate-General for Maritime Affairs and FisheriesE-MODnet Digital Bathymetry. 2018, Available online: http://data.europa.eu. [Accessed on 28 April 2022].
[31] Díaz H, Fonseca RB, Guedes Soares C. Site selection process for floating offshore wind farms in madeira islands. In: Advances in renewable energies offshore. London: Taylor & Francis Group; 2019.
[32] Ryberg D, Robinius M, Stolten D. Methodological framework for determining the land eligibility of renewable energy sources. 2017.
[33] European Marine Observation and Data Network. Data services. 2022, Available online: https://www.emodnet-humanactivities.eu/search.php. [Accessed on 3 May 2022].
[34] European Commission, Directorate-General for Maritime Affairs and Fisheries. Unlocking seabed habitat data in europe. 2021, Available online: https://www.emodnet-seabedhabitats.eu/. [Accessed on 28 April 2022].
[35] Maienza C, Avossa AM, Ricciardelli F, Coiro D, Georgakis CT. Sensitivity analysis of cost parameters for floating offshore wind farms: an application to Italian waters. J Phys Conf Ser 2020. http://dx.doi.org/10.1088/1742-6596/1669/1/012019.
[36] UK Maritime and Coastguard Agency. Offshore renewable energy installations safety response. Technical report MGN 654 (M+F), National Renewable Energy Laboratory; 2021.
[37] Argyle P, Watson S. Offshore turbine wake power losses: Is turbine separation significant? Energy Procedia 2017. http://dx.doi.org/10.1016/j.egypro.2017.10.340.
[38] Division for Ocean Affairs and the Law of the Sea. United nations convention on the law of the sea. Technical report, United Nations; 2022.
[39] Mike Clare, ICPCMarine Environmental Adviser. Submarine cable protection and the environment - An update from the ICPC. Technical report issue 4, The International Cable Protection Committee; 2022.
[40] Global Wind Atlas. Bathymetry terrain layer. OpenStreetMap; 2021, Available online: https://globalwindatlas.info/. [Accessed on 26 April 2022].
[41] Vestas Wind Systems A/S. 4 MW platform. Brochure, Vestas Group; 2022, Available online: https://www.vestas.com/en/products/4-mw-platform/4-mw-platform. [Accessed on 18 April 2022].
[42] Walsh SD, Easton L, Weng Z, Wang C, Moloney J, Feitz A. Evaluating the economic fairways for hydrogen production in Australia. Int J Hydrog Energy 2021. http://dx.doi.org/10.1016/j.ijhydene.2021.08.142.
[43] Geoscience Australia. AusH2 - Australia's hydrogen opportunities tool. 2021, Available online: https://portal.ga.gov.au/persona/heft. [Accessed on 03 July 2022].
[44] Vartiainen E, Masson G, Breyer C, Moser D, Román Medina E. Impact of weighted average cost of capital, capital expenditure, and other parameters on future utility-scale PV levelised cost of electricity. Prog Photovolt, Res Appl 2020. http://dx.doi.org/10.1002/pip.3189.
[45] Rubert T, McMillan D, Niewczas P. A decision support tool to assist with lifetime extension of wind turbines. Renew Energy 2018. http://dx.doi.org/10.1016/j.renene.2017.12.064.
[46] de Novaes Pires Leite G, Weschenfelder F, de Farias JG, Kamal Ahmad M. Economic and sensitivity analysis on wind farm end-of-life strategies. Renew Sustain Energy Rev 2022. http://dx.doi.org/10.1016/j.rser.2022.112273.
[47] Trading Economics. Euro area inflation rate. 2022, Available online: https://tradingeconomics.com/euro-area/inflation-cpi. [Accessed on 04 August 2022].
[48] Steffen B. Estimating the cost of capital for renewable energy projects. Energy Econ 2020. http://dx.doi.org/10.1016/j.eneco.2020.104783.
[49] Minutillo M, Perna A, Forcina A, Di Micco S, Jannelli E. Analyzing the levelized cost of hydrogen in refueling stations with on-site hydrogen production via water electrolysis in the Italian scenario. Int J Hydrog Energy 2021. http://dx.doi.org/10.1016/j.ijhydene.2020.11.110.

[50] Viktorsson L, Heinonen JT, Skulason JB, Unnthorsson R. A step towards the hydrogen economy—A life cycle cost analysis of a hydrogen refueling station. Energies 2017. http://dx.doi.org/10.3390/en10060763.
[51] International Renewable Energy Agency and International Energy Agency Photovoltaic Power Systems. End-of-life management: Solar photovoltaic panels. Technical report, International Renewable Energy Agency and IEA-PVPS; 2016.
[52] Giovannini G. Wind farm decommissioning: a perspective on regulations and cost assessment in italy and sweden. [Master's thesis], Uppsala University; 2014.
[53] Department for Business, Energy and Industrial Strategy. Hydrogen production costs 2021. Technical guide, UK: BEIS; 2021.
[54] Lehner F, Hart D. Chapter 1 - the importance of water electrolysis for our future energy system. In: Electrochemical power sources: fundamentals, systems, and applications. Elsevier; 2022, http://dx.doi.org/10.1016/B978-0-12-819424-9.00008-2.
[55] Gigastack. Gigastack phase 2: pioneering UK renewable hydrogen. Public report, Gigastack; 2019.
[56] NEL. PEM electrolyser specifications. 2022, Available online: https://nelhydrogen.com/product/m-series-3/. [Accessed on 06 August 2022].
[57] Cummins. Hylyzer water electrolyzers. 2022, Available online: https://www.cummins.com/sites/default/files/2021-08/cummins-hylyzer-1000-specsheet.pdf. [Accessed on 06 August 2022].
[58] Power P. The plug EX-425d. 2022, Available online: https://www.plugpower.com/hydrogen/electrolyzer-hydrogen/electrolyzer-products/. [Accessed on 06 August 2022].
[59] Siemens Energy. Silyzer 300. 2022, Available online: https://www.siemens-energy.com/global/en/offerings/renewable-energy/hydrogen-solutions.html. [Accessed on 06 August 2022].
[60] Solar C. Bifacial high power dual cell PERC module. 2022, Available online: https://www.csisolar.com/bihiku7/. [Accessed on 09 August 2022].
[61] Mahachi T, Rix A. Energy yield analysis and evaluation of solar irradiance models for a utility scale solar PV plant in South africa [Ph.D. thesis], Stellenbosch University; 2016, http://dx.doi.org/10.13140/RG.2.2.19638.45127.
[62] Global Wind Atlas. (November 2018 release note). GWA 2.3; 2022, Available online: https://globalwindatlas.info/about/ReleaseNotes. [Accessed on 13 April 2022].
[63] Clayton D. Wind turbine spacing: how far apart should they be?. Energy Follower; 2022, Available online: https://energyfollower.com/wind-turbine-spacing/. [Accessed on 10 August 2022].
[64] Gaughan R. How much land is needed for wind turbines?. 2018, Available online: https://sciencing.com/much-land-needed-wind-turbines-12304634.html. [Accessed on 10 August 2022].
[65] Duval G. How many wind turbines can fit on one acre?. 2021, Available online: https://www.semprius.com/how-much-space-does-a-wind-turbine-need/. [Accessed on 10 August 2022].
[66] Global Solar Atlas. Map and data downloads: Italy. 2021, Available online: https://globalsolaratlas.info/download/italy. [Accessed on 10 April 2022].
[67] Global Solar Atlas. Map and data downloads: Portugal. 2021, Available online: https://globalsolaratlas.info/download/portugal. [Accessed on 10 April 2022].
[68] Global Wind Atlas. Mean wind speed: Italy. OpenStreetMap; 2021, Available online: https://globalwindatlas.info/area/Italy. [Accessed on 10 April 2022].
[69] Global Wind Atlas. Mean wind speed: Portugal. OpenStreetMap; 2021, Available online: https://globalwindatlas.info/area/Portugal. [Accessed on 10 April 2022].
[70] Hart WE, Watson J-P, Woodruff DL. Pyomo: modeling and solving mathematical programs in python. Math Program Comput 2011.
[71] Bynum ML, Hackebeil GA, Hart WE, Laird CD, Nicholson BL, Siirola JD, et al. 3rd ed.. Pyomo–optimization modeling in Python, vol. 67, Springer Science & Business Media; 2021.
[72] Huld T, Müller R, Gambardella A. A new solar radiation database for estimating PV performance in europe and africa. Sol Energy 2012. http://dx.doi.org/10.1016/j.solener.2012.03.006.
[73] Pfenninger S, Staffell I. Long-term patterns of European PV output using 30 years of validated hourly reanalysis and satellite data. Energy 2016. http://dx.doi.org/10.1016/j.energy.2016.08.060, Available online: https://www.renewables.ninja. [Accessed on 14 August 2022].
[74] Staffell I, Pfenninger S. Using bias-corrected reanalysis to simulate current and future wind power output. Energy 2016. http://dx.doi.org/10.1016/j.energy.2016.08.068, Available online: https://www.renewables.ninja. [Accessed on 14 August 2022].